

## Mechanisms of Tropical Pacific Decadal Variability

Antionietta Capotondi<sup>1,2,†</sup>, Shayne McGregor<sup>3,4</sup>, Michael J. McPhaden<sup>5</sup>, Sophie Cravatte<sup>6,7</sup>,  
Neil J. Holbrook<sup>8,9</sup>, Yukiko Imada<sup>10</sup>, Sara C. Sanchez<sup>11</sup>, Janet Sprintall<sup>12</sup>, Malte F.  
Stuecker<sup>13,14</sup>, Caroline C. Ummerhofer<sup>15,16</sup>, Mathias Zeller<sup>17</sup>, Riccardo Farneti<sup>18</sup>, Giorgio  
Graffino<sup>19</sup>, Shijian Hu<sup>20</sup>, Kristopher B. Karnauskas<sup>11,1</sup>, Yu Kosaka<sup>21</sup>, Fred Kucharski<sup>18</sup>,  
Michael Mayer<sup>22,23</sup>, Bo Qiu<sup>13</sup>, Agus Santoso<sup>24,16</sup>, Andréa S. Taschetto<sup>24,16</sup>, Fan Wang<sup>20</sup>,  
Xuebin Zhang<sup>25</sup>, Ryan M. Holmes<sup>26</sup>, Jing-Jia Luo<sup>27</sup>, Nicola Maher<sup>1,11,28</sup>, Cristian Martinez-  
Villalobos<sup>29,30</sup>, Gerald, A. Meehl<sup>31</sup>, Rajashree Naha<sup>3</sup>, Niklas Schneider<sup>13,14</sup>, Samantha  
Stevenson<sup>32</sup>, Arnold Sullivan<sup>33</sup>, Peter van Rensch<sup>3</sup>, Tongtong Xu<sup>1,2</sup>

1. Cooperative Institute for Research in Environmental Sciences, University of Colorado, Boulder, CO, USA.
2. NOAA/Physical Sciences Laboratory, Boulder, CO, USA
3. School of Earth Atmosphere and Environment, Monash University, Clayton, VIC, Australia.
4. ARC Centre of Excellence for Climate Extremes, Monash University, Clayton, VIC, Australia.
5. NOAA/Pacific Marine Environmental Laboratory, Seattle, WA, USA.
6. LEGOS, Université de Toulouse, IRD, CNES, CNRS, UPS, Toulouse, France.
7. IRD, Nouméa, New Caledonia.
8. Institute for Marine and Antarctic Studies, University of Tasmania, Hobart, TAS Australia.
9. ARC Centre of Excellence for Climate Extremes, University of Tasmania, Hobart, 7001, Tasmania, Australia.
10. Meteorological Research Institute, Tsukuba, Japan.
11. Department of Atmospheric and Oceanic Sciences, University of Colorado Boulder, Boulder, CO, USA.
12. Scripps Institution of Oceanography, University of California, San Diego, La Jolla, USA.
13. Department of Oceanography, School of Ocean and Earth Science and Technology (SOEST), University of Hawai‘i at Mānoa, Honolulu, HI, USA.
14. International Pacific Research Center (IPRC), School of Ocean and Earth Science and Technology (SOEST), University of Hawai‘i at Mānoa, Honolulu, HI, USA.
15. Department of Physical Oceanography, Woods Hole Oceanographic Institution, Woods Hole, MA, USA.
16. ARC Centre of Excellence for Climate Extremes, University of New South Wales, Sydney, New South Wales, Australia.
17. GEOMAR Helmholtz Centre for Ocean Research, Kiel, Germany.
18. Abdus Salam International Centre for Theoretical Physics, Trieste, Italy.
19. National Centre for Atmospheric Science, Department of Meteorology, University of Reading, Reading RG6 6ET, United Kingdom.
20. 20 CAS Key Laboratory of Ocean Circulation and Waves, Institute of Oceanology, Chinese Academy of Sciences, Qingdao 266071, Shandong, China.
21. Research Center for Advanced Science and Technology, The University of Tokyo, Tokyo, Japan.
22. Research Department, European Centre for Medium-Range Weather Forecasts, Reading, UK.
23. Department of Meteorology and Geophysics, University of Vienna, Vienna, Austria.
24. Climate Change Research Centre, The University of New South Wales, Sydney, NSW, Australia.
25. Climate Science Centre, CSIRO Environment, Hobart, Tasmania, Australia.
26. School of Geosciences, The University of Sydney, Sydney, Australia.
27. Institute of Climate Application Research (ICAR)/CIC-FEMD, Nanjing University of Information Science & Technology, Nanjing, China.
28. Research School of Earth Sciences and ARC Centre of Excellence for Climate Extremes, Australian National University, Canberra, ACT, Australia
29. Faculty of Engineering and Science, Universidad Adolfo Ibáñez, Peñalolén, Santiago, Chile.
30. Data Observatory Foundation, Santiago, Chile.
31. National Center for Atmospheric Research, Boulder, CO, USA
32. Bren School of Environmental Science and Management, University of California, Santa Barbara, CA, USA
33. CSIRO Oceans and Atmosphere, 107–121 Station Street, Aspendale, VIC 3195, Australia.

†email: [antionietta.capotondi@noaa.gov](mailto:antionietta.capotondi@noaa.gov)

59 **Abstract**

60

61 Naturally-occurring tropical Pacific variations at timescales of 7-70 years—Tropical Pacific  
62 Decadal Variability (TPDV)—describe basin-scale sea surface temperature (SST), sea level  
63 pressure and heat content anomalies. Several mechanisms are proposed to explain TPDV,  
64 which can originate through oceanic processes, atmospheric processes, or as an ENSO residual.  
65 In this Review, we synthesise knowledge of these mechanisms, their characteristics and  
66 contribution to TPDV. Oceanic processes include off-equatorial Rossby waves, which mediate  
67 oceanic adjustment and contribute to variations in equatorial thermocline depth and SST;  
68 variations in the strength of the shallow upper-ocean overturning circulation, which exhibit a  
69 large anti-correlation with equatorial Pacific SST at interannual and decadal timescales; and  
70 the propagation of salinity-compensated temperature (“spiciness”) anomalies from the  
71 subtropics to the equatorial thermocline. Atmospheric processes include midlatitude internal  
72 variability inducing (sub)tropical wind anomalies, which result in equatorial SST anomalies,  
73 and in atmospheric feedbacks that enhance persistence; and atmospheric teleconnections from  
74 Atlantic and Indian Ocean SST variability, which induce winds conducive to decadal anomalies  
75 of the opposite sign in the Pacific. Although uncertain, the tropical adjustment through Rossby  
76 wave activity is likely a dominant mechanism. A deeper understanding of the origin and  
77 spectral characteristics of TPDV-related winds is a key priority.

78

79

80 **Key points**

81

- 82 • Tropical Pacific decadal variations are linked to basin-scale sea surface temperature  
83 and sea level pressure anomalies, and are associated with a zonal reorganization of  
84 tropical Pacific heat content.
- 85 • Salinity-compensated temperature anomalies (“spiciness anomalies”) can reach the  
86 equatorial thermocline, but their amplitude appears small and their influence on  
87 equatorial sea surface temperatures remains uncertain.
- 88 • Variability of the Pacific upper-ocean overturning circulation exhibits a large anti-  
89 correlation with equatorial Pacific SSTs at both interannual and decadal timescales,  
90 suggesting that similar mechanisms are operating at both timescales.
- 91 • Internally generated subtropical/tropical wind anomalies can create equatorial SST  
92 anomalies, which in turn can reinforce the wind anomalies locally and through  
93 atmospheric teleconnections to increase their persistence.
- 94 • Decadal SST anomalies in the Atlantic and Indian Oceans can induce wind anomalies  
95 in the tropical Pacific conducive to the formation of decadal SST anomalies of the  
96 opposite sign.

97

98

99 **Introduction**

100

101 The tropical Pacific exhibits variability over a broad range of timescales from seasonal to  
102 centennial. While the El Niño Southern Oscillation (ENSO) is the dominant mode of variability  
103 at interannual timescales (about 2-7 years), “natural” variations arising from processes internal  
104 to the climate system are also observed in the “decadal” range, namely at timescales longer  
105 than the ENSO timescales, but shorter than the centennial trend resulting from anthropogenic  
106 forcing. Internal variations at periods longer than 7 years can occur at both quasi-decadal and  
107 multi-decadal timescales<sup>1</sup>, and hence we define Tropical Pacific Decadal Variability (TPDV)  
108 as variability in the 7-70 years range.

109  
110 TPDV is the tropical expression of large-scale patterns of variability like the Pacific Decadal  
111 Oscillation (PDO)<sup>2</sup> in the North Pacific, and the Interdecadal Pacific Oscillation (IPO)<sup>3</sup> over  
112 the entire Pacific basin. The positive phase of TPDV is characterized by warm SSTAs in the  
113 tropical Pacific, and along the western coasts of the Americas, and by negative anomalies in  
114 the central/western midlatitudes of both hemispheres, while the negative TPDV phase exhibits  
115 SSTAs of the opposite sign.

116  
117 Such TPDV could just result as a residual of interannual ENSO variability<sup>4</sup>, but various oceanic  
118 and atmospheric processes could also produce variability at decadal timescales, with important  
119 implications for the potential predictability of TPDV. Since the equatorial Pacific is connected  
120 to the subtropics through an oceanic pathway (Box 1), temperature anomalies created in the  
121 subtropics can reach the equatorial pycnocline and be brought to the surface by equatorial  
122 upwelling, a mechanism known as the “ $\bar{v}T'$  hypothesis”, with  $\bar{v}$  indicating the time mean  
123 circulation and  $T'$  the temperature anomaly. Alternatively, changes in the ocean circulation  
124 could result in equatorial SSTAs through changes in equatorial upwelling (Box 1), a  
125 mechanism termed the “ $v'\bar{T}$  hypothesis”. These oceanic changes are part of a slow oceanic  
126 adjustment to atmospheric variability, which is mediated by oceanic wave activity occurring at  
127 decadal timescales. Atmospheric processes include influences from the extratropical Pacific,  
128 atmospheric response to equatorial SSTAs, and interactions with the Atlantic and Indian  
129 Oceans. However, no consensus exists on the effectiveness and relative importance of these  
130 processes.

131  
132 TPDV modulates ENSO characteristics<sup>5,6</sup> and some of its global impacts<sup>4,7,8</sup>, and has been  
133 linked to the rate of change of the globally-averaged surface temperature<sup>9,10</sup>. Thus, the ability  
134 to predict the occurrence of different decadal epochs in the tropical Pacific has important  
135 societal implications, which has motivated the development of major decadal prediction efforts  
136 in several centres around the world. However, TPDV predictability remains elusive, hence the  
137 need to better understand its underlying mechanisms. A better understanding of TPDV is also  
138 needed to more robustly separate the forced climate response from internally-generated climate  
139 variability and to achieve more reliable future projections of tropical Pacific climate, which has  
140 implications for the global climate<sup>9</sup>. Some climate models used for both predictions and  
141 projections appear to underestimate internally-generated decadal variations<sup>11-13</sup>. Although this  
142 conclusion may be severely hampered by the relatively short duration of the observational  
143 record, as indicated by paleoclimate data (Box 2), an assessment of model fidelity in  
144 realistically reproducing the relevant mechanisms of decadal variability is essential.

145  
146 In this Review, we critically synthesise the current state-of-knowledge of the mechanisms  
147 proposed for TPDV, based on observations, ocean reanalyses, dynamical models, and  
148 paleoclimate evidence. Relative to other reviews on this topic<sup>4</sup>, which have considered both  
149 internal and anthropogenically-forced low-frequency variability, this synthesis focuses on  
150 *internal* decadal variations in order to allow for in-depth developments of the key concepts.  
151 We will describe salient features of TPDV in the context of the decadal phase transition that  
152 occurred in the late 1990s, followed by a description of the leading oceanic and atmospheric  
153 processes relevant for TPDV. We end with recommendations for future research and some  
154 hypotheses on how TPDV may change in a warmer world.

155  
156  
157  
158

## 159 **Observed tropical Pacific decadal changes**

160

161 Before reviewing the mechanisms proposed to explain TPDV, it is important to identify the  
162 key oceanic and atmospheric changes accompanying decadal phase transitions. To illustrate  
163 such changes, we consider the dramatic shift to colder equatorial SSTs that occurred during  
164 1999-2014 relative to 1984-1999, concurrent with phase transitions of both the PDO and IPO.  
165 The spatial structure of these SST changes (Fig. 1a, shading) is characterized by cold conditions  
166 in the equatorial Pacific, and warm anomalies in the central/western midlatitudes. This pattern  
167 is similar to that obtained through a statistical definition of TPDV, as the leading EOF of 7-70  
168 years band-pass filtered SSTAs in the tropical Pacific (25°S-25°N). The basin-wide TPDV  
169 pattern is then determined through linear regression of SSTAs on the associated principal  
170 component--the TPDV index (Fig. 1a, contours). The decadal SST pattern in the tropical  
171 Pacific is “ENSO-like”, but with a broader meridional extent and with the largest equatorial  
172 variability shifted further west than the interannual ENSO variance<sup>4,14</sup>. The large-scale SST  
173 changes from 1984-1999 to 1999-2014 are accompanied by sea level pressure anomalies in the  
174 extra-tropics of both hemispheres (Fig. 1b), and by wind anomalies that include an  
175 enhancement of the easterly trade winds in the tropics.

176

177 This trade wind intensification has led to changes in the ocean density structure and  
178 circulation<sup>15,16</sup>, resulting in a reorganization of the tropical Pacific heat content<sup>11,17</sup>. Such  
179 reorganization is captured by the changes in SSH (Fig. 1c), a quantity dynamically linked to  
180 upper ocean heat content and thermocline depth. Positive SSH differences (higher heat content,  
181 deeper thermocline) occur in the western tropical Pacific, with maxima located off the equator,  
182 while negative SSH differences (reduced heat content, shallower thermocline) are found in the  
183 central and eastern part of the basin. These SSH differences are consistent with the SSH  
184 signature of TPDV (Fig. 1c, contours), and are also consistent with typical SSH decadal  
185 patterns<sup>1</sup>. Increased heat content is seen in the western tropical Pacific at the depth of the  
186 thermocline (Fig. 1e), and is primarily associated with westward-propagating Rossby waves<sup>18</sup>,  
187 while decreased heat content is found in the upper ocean east of the dateline (Fig. 1f). Oceanic  
188 changes during negative-to-positive decadal transitions largely mirror the surface and  
189 subsurface changes shown here<sup>18,19</sup>. Positive SSH anomalies are also present in the Indonesian  
190 Seas and eastern Indian Ocean (Box 1), suggesting a transfer of heat from the Pacific to the  
191 Indian Ocean in conjunction with negative TPDV phases<sup>20,21</sup>. Indeed, the Indian Ocean heat  
192 content exhibits a decadal modulation that is in phase with Pacific decadal variations, likely  
193 associated with changes in the western Pacific winds and their influence on the transport of the  
194 Indonesian Throughflow (ITF, Box1)<sup>22-24</sup>.

195

196 The decadal transition after 1999 occurred in the presence of tropical trends<sup>11</sup> (Fig. 1b), which  
197 are particularly pronounced in the SSH field<sup>25-27</sup> (Fig. 1c, d). This SSH trend seems to have  
198 accelerated since 2000<sup>21</sup>, and is particularly evident in the western Pacific, Indonesian Seas and  
199 eastern Indian Ocean (Fig. 1d), as a result of the tropical easterly surface trade wind  
200 intensification. This wind intensification and the zonal SSH gradient are not captured by state-  
201 of-the-art climate models, introducing a large uncertainty in the attribution of the trend to either  
202 internal low-frequency variability or to climate change<sup>24,28-30</sup>. This ambiguity highlights the  
203 importance of a deepened understanding of internal low-frequency variability for robustly  
204 separating the two components.

205

206 To that end, we now revisit the leading mechanisms proposed for TPDV. We first discuss the  
207 possibility that TPDV arises as a residual of interannual ENSO variations, and then consider  
208 mechanisms involving oceanic and atmospheric processes, including the  $\bar{v}T'$  and the  $v'\bar{T}$

209 hypotheses, as well as the atmospheric influences from the extra-tropics and from the Atlantic  
210 and Pacific Oceans. The pattern of TPDV that emerges from a statistical EOF approach (Fig.  
211 1a, contours) of anomalies spanning a broad range of timescales (7-70 years) does not presume  
212 that a single set of dynamically-related physical processes is responsible for it, as demonstrated  
213 for the PDO, which results from the combination of different dynamical modes with different  
214 timescales<sup>31</sup>. The purpose of this paper is to elucidate the nature and relative importance of  
215 these processes.

216

### 217 **TPDV as an ENSO residual**

218

219 Since the tropical Pacific climate is dominated by interannual ENSO variations, a plausible  
220 hypothesis is that TPDV arises as a residual of ENSO. Indeed, the “ENSO-like”<sup>14</sup> spatial  
221 pattern of TPDV can be reconstructed from decadal averages of evolving ENSO patterns, from  
222 their developing to decaying phases, and random event-to-event variations of those patterns<sup>4,32</sup>.  
223 In addition, uneven numbers of warm (El Niño) or cold (La Niña) events, can randomly occur  
224 during different decadal epochs (Fig. 2a), resulting in El Niño-like, or La Niña-like decadal  
225 conditions because of the differences in amplitude and spatial asymmetry of ENSO events.  
226 Also, uneven numbers of events with largest anomalies centered either in the Eastern (EP) or  
227 Central (CP) Pacific<sup>33</sup> (Fig. 2a) can contribute to low-frequency background changes<sup>34</sup>. Similar  
228 to the influence of stochastic sub-seasonal disturbances on the development of El Niño<sup>35,36</sup>,  
229 ENSO events could also act as triggers for TPDV phase transitions, either through changes of  
230 off-equatorial winds responsible for discharging the heat content anomalies in the western  
231 Pacific<sup>37</sup>, or through low-frequency equatorial Pacific changes induced by nonlinear dynamical  
232 heating<sup>38</sup>. Off-equatorial western Pacific heat content anomalies (Fig. 1c) are a necessary  
233 condition for an ENSO event to trigger a TPDV transition<sup>37,39</sup>.

234

235 The interpretation of TPDV as an ENSO residual also involves subsurface anomalies. Western  
236 Pacific heat content exhibits a decadal modulation, with a reduced heat content during periods  
237 of positive TPDV (prevailing negative anomalies during 1976-1999 in Fig. 2c, when the TPDV  
238 index in Fig. 2d is predominantly positive) and *vice versa* (prevailing positive anomalies during  
239 1999-2014 in Fig. 2b, associated with a predominantly negative TPDV). These low-frequency  
240 variations are punctuated by the heat content changes associated with the recharge-discharge  
241 activity of individual ENSO events (Fig. 2b), which are the dominant signal in the eastern part  
242 of the basin (Fig. 2c). The decadal modulation of tropical Pacific heat content could thus be  
243 interpreted as the low-frequency envelope of interannual ENSO variations.

244

245 However, ENSO characteristics also depend upon the mean state<sup>40,41</sup>. The warm phase of  
246 TPDV, characterized by weaker trade winds and a deeper thermocline in the eastern equatorial  
247 Pacific, favours more frequent and stronger El Niño events of EP-type, as seen during 1976-  
248 1999 (Fig. 2a, warm anomalies extending to the far-eastern part of the basin), while negative  
249 TPDV phases, like the 1999-2014 period, are characterized by weaker El Niño events with  
250 peak anomalies in the central Pacific (Fig. 2a). Dynamical model sensitivity experiments have  
251 indeed highlighted the impact of the initial background conditions on ENSO evolution and  
252 predictive skill<sup>42,43</sup>. The decadal modulation of ENSO, as captured in climate models by the  
253 second EOF of decadal SSTAs<sup>5,44,45</sup> is significantly lag-correlated with TPDV<sup>45</sup>, with a large  
254 inter-model dependence<sup>44</sup>. ENSO decadal modulation appears to lead the opposite phase of  
255 TPDV by about two years, suggesting its possible role as precursor of TPDV phase  
256 transitions<sup>45</sup>. However, TPDV also leads the same phase of ENSO decadal modulation by two  
257 years with a higher correlation<sup>45</sup>, indicating that ENSO modulation by TPDV may be more  
258 prominent than the influence of ENSO activity on TPDV.

259  
260  
261  
262  
263  
264  
265  
266  
267  
268  
269  
270  
271  
272  
273  
274  
275  
276  
277  
278  
279  
280  
281  
282  
283  
284  
285  
286  
287  
288  
289  
290  
291  
292  
293  
294  
295  
296  
297  
298  
299  
300  
301  
302  
303  
304  
305  
306  
307  
308

## The $\bar{v} T'$ hypothesis and wave processes

The  $\bar{v} T'$  hypothesis considers the effect of equatorward advection of temperature anomalies within the pycnocline as a driver of TPDV (Fig. 3a). This mechanism was originally proposed for anomalies that leave the surface mixed layer to enter the subsurface ocean in the northern mid-latitudes<sup>46</sup>, and are advected by the mean circulation (the northern subsurface branches of the STC, Box1) toward the equator, where they are upwelled to the surface, altering SSTs and leading to a change of the TPDV phase. However, observational and modelling results based on temperature observations only showed that these anomalies decayed prior to reaching the equator<sup>47</sup>, casting doubt on the feasibility of this mechanism. Further works suggested that the South Pacific could be more suitable for the  $\bar{v} T'$  mechanism<sup>48-50</sup>, due to its larger and more direct equatorward transport<sup>51-54</sup>. Indeed, the presence of the Intertropical Convergence Zone (ITCZ) in the tropical North Pacific alters the depth of the pycnocline and creates a “potential vorticity barrier”<sup>54</sup> that limits the interior equatorward flow<sup>54,55</sup> (Fig. 3).

Moreover, a more careful examination of the mechanisms by which subtropical signals reach the equator highlighted two different types of mechanisms: spiciness anomalies advected as passive tracer by the mean circulation, and non-compensated temperature anomalies propagating as planetary waves.

### *Advection of spiciness anomalies*

Ocean density increases with decreasing temperature and increasing salinity. Temperature anomalies with a density compensating salinity signal (“spiciness anomalies”<sup>56</sup>), do not affect density and can propagate along isopycnals as a passive tracer<sup>57</sup> (Fig. 3a). These warm-salty or cold-fresh anomalies appear to be predominantly generated in the eastern subtropics of the Pacific basin<sup>58,59</sup> through either shifts in spiciness gradients induced by wind-forced anomalous ocean currents<sup>57</sup>, or through buoyancy-forced penetrative mixing<sup>59</sup>. At large spatial scales, theoretical arguments suggest that pycnocline advection may result in a frequency spectrum of spiciness anomalies reaching the equator that has enhanced power in the decadal range<sup>60</sup>. Based on fully coupled model experiments<sup>57,61</sup> a mechanism for TPDV was proposed, in which spiciness anomalies generated in the off-equatorial regions by changes in the tropical trade winds are advected toward the equator, where they are upwelled to the surface, rearrange equatorial sea surface temperatures, winds and the slope of the pycnocline (Box 1)<sup>61</sup>, and induce off-equatorial atmospheric forcing of spiciness anomalies of the opposite sign, resulting in a 10-year cycle.

Spiciness generation and pathways from the eastern subtropics towards the western tropical Pacific are supported by observations<sup>62-67</sup>. Observations also show that spiciness anomalies undergo some decay during their propagation to the tropical region<sup>65,67,68</sup>. However, whether these anomalies are advected all the way to the equator and reach the surface at the equator is much less clear. The complexity of the LLWBCs and the high level of mixing and water mass transformation occurring in some parts of these swift currents<sup>69</sup> cast doubt on the feasibility of a western boundary pathway. Modelling results using a Lagrangian approach however suggest that spiciness anomalies can reach the eastern equatorial band<sup>55</sup>, with a clear dominance of southern hemisphere pathways. A heat budget analysis of the modelled equatorial Pacific mixed layer reveals a potential influence of spiciness anomalies on TPDV<sup>68</sup>, yet with a small magnitude, leaving the efficiency of this mechanism unclear.

310

311 Oceanic Rossby waves cause isopycnal displacements that appear as temperature anomalies  
 312 over time-mean isopycnal surfaces. Rossby wave activity has been related to decadal  
 313 subsurface temperature anomalies in the tropical Pacific with maxima around 10°-15°N and  
 314 10°-14°S<sup>18,48,49,70-72</sup> (Fig. 2c). These anomalies can reach the equatorial thermocline via the  
 315 western boundary and propagate eastward along the equator as equatorial Kelvin waves  
 316 altering equatorial SSTs. However, the origin of the decadal timescale remains unclear since  
 317 the Rossby wave transit time at the latitudes of the Rossby wave maxima is only 2-3 years. One  
 318 hypothesis is that the latitudes of the Rossby wave maxima coincide with areas of high zonal  
 319 coherence of the wind forcing, which may be more efficient in exciting larger amplitude waves  
 320 at decadal timescales<sup>71</sup>. In addition, these latitudes coincide with the equatorward boundaries  
 321 of the subtropical gyres, where instability processes may energize planetary waves originating  
 322 in the eastern midlatitudes of both hemispheres with longer transit times in the decadal range<sup>72</sup>.  
 323 Finally, equatorial signals have a slow eastward propagation due to the coupling of the oceanic  
 324 waves with the local winds<sup>48</sup>. More generally, decadal timescales cannot be expected to  
 325 coincide with the transit time of one single wave, but result from the collective effect of  
 326 multiple waves generated over relatively broad latitude bands at different times, which may  
 327 lead to a longer adjustment timescale.

328

329 Coupled climate model experiments suggest that a mix of both advection and planetary wave  
 330 activity contributes to the equatorward propagation of temperature anomalies with a potentially  
 331 larger impact of anomalies from the Southern Hemisphere<sup>49,50</sup>. CGCM sensitivity experiments,  
 332 where oceanic temperature and salinity anomalies were blocked from reaching the equator in  
 333 both hemispheres, indicated that the southern  $\bar{v} T'$  process acts as a delayed negative feedback  
 334 for bi-decadal (12-25yr) variability, whereas oceanic wave adjustment has a dominant  
 335 influence in the decadal range (9-12yr)<sup>50</sup>. The role of decadal anomalies from the South Pacific  
 336 was further illustrated by their influence on the evolution of El Niño events during the first  
 337 decade of the 2000s, as noted in decadal prediction experiments<sup>73</sup>. Cold anomalies in the  
 338 southwestern tropical Pacific related to the negative TPDV phase during 1999-2014 may have  
 339 impacted the development of El Niño events<sup>73</sup>, possibly leading to the unexpected termination  
 340 of El Niño in 2014<sup>74</sup>.

341

342

### 343 **The $\bar{v}T'$ hypothesis**

344

345 Changes in the strength of the STCs' transport (Fig. 3b) can affect equatorial upwelling and  
 346 equatorial SSTs. Specifically, an increase in the STCs' equatorward mass transport will induce  
 347 enhanced equatorial upwelling, bringing colder pycnocline waters closer to the surface and  
 348 cooling the equatorial SSTs, while reduced STC transport will result in warmer SSTs<sup>75</sup>.  
 349 Originally illustrated in the context of simple models<sup>75-78</sup>, this hypothesis has also been  
 350 extensively tested in observations<sup>19,79</sup>, ocean general circulation models<sup>80-83</sup> and ocean  
 351 reanalyses<sup>18,84</sup>. The pycnocline flow, zonally averaged east of the LLWBCs ("interior  
 352 transport" hereafter)<sup>19</sup> is used as a measure of the STCs' strength. Since 9°N is a choke point  
 353 for the equatorward flow (Fig. 3b), this latitude has been chosen to estimate the interior  
 354 transport in the Northern Hemisphere, and 9°S is used in the Southern Hemisphere for  
 355 equatorial symmetry<sup>19</sup>. Observational estimates of the interior transports at these two latitudes  
 356 over the second half of the 20<sup>th</sup> century show a decline of the equatorward subsurface mass  
 357 convergence after the mid-seventies, which was concurrent with the tropical Pacific warming  
 358 associated with the "1976-77 climate shift"<sup>2,19</sup>(Fig. 4a, b).

359  
360 Due to the sparsity of subsurface observations,<sup>19</sup> binned the data over multi-year periods to  
361 obtain transport estimates (Fig. 4a, b). Ocean reanalyses and ocean models forced by  
362 observationally-constrained surface fields allowed transport estimates at a higher time  
363 resolution and confirmed that increased interior equatorward mass convergence is associated  
364 with colder equatorial SSTs, and *vice versa* (Fig. 4c, d), with high correlations at both  
365 interannual and decadal timescales<sup>18,80,84</sup> (Fig. 5c, d). Changes in interior transport at  
366 interannual timescales encapsulate the recharge/discharge of the equatorial upper-ocean heat  
367 content, underpinning ENSO evolution<sup>85</sup>. The relationship between transport convergence and  
368 SST anomalies at decadal timescales suggests that similar underlying dynamics may be at play  
369 also at lower frequencies<sup>86</sup>.

370  
371 Many climate models also show correlations between transport convergence and SST  
372 anomalies that are comparable with those obtained from ocean reanalyses (Fig. 4e), although  
373 some models exhibit much weaker relationships<sup>87,88</sup>. In addition, the transport variability is  
374 generally weaker in the models than in observations for the same SST variability (Fig. 4f)<sup>87,88</sup>,  
375 suggesting a higher sensitivity of modelled SSTs to STC variability.

376  
377 The total equatorward pycnocline transport includes both the interior transport and the transport  
378 of the LLWBCs. LLWBCs' transport anomalies are of the opposite sign to the interior transport  
379 anomalies in both models and observational estimates<sup>80,89-91</sup>, leading to a partial compensation  
380 of the interior mass convergence. The sign of the boundary transport anomalies has been related  
381 to the development of anomalous gyre circulations in the western tropical Pacific, as implied  
382 by the SSH anomalies in Fig. 1c for the negative TPDV phase, with a clockwise (anticlockwise)  
383 circulation in the Northern (Southern) Hemisphere<sup>15,18,79</sup>. Given the complexity of the  
384 LLWBCs, and the sparsity of in situ observations in these regions, it is unclear whether  
385 numerical models can realistically simulate these currents and what fraction of their anomalous  
386 transport recirculates in the western Pacific, exits the Pacific through the ITF or acts to alter  
387 the equatorial mass balance.

388  
389 The strength of the ITF can also contribute to the mass and heat balance of the equatorial  
390 Pacific<sup>92</sup>, as seen in the case of the two extreme El Niño events of 1997/98 and 2015/16, whose  
391 difference in ocean heat discharge was controlled by different strengths of the ITF<sup>93,94</sup>. On  
392 interannual timescales, variations in the ITF strength are related to the SSH difference between  
393 the western Pacific and eastern Indian Ocean, as well as buoyancy forcing<sup>24,95</sup>. They likely also  
394 respond to slow changes in the large-scale SSH and salinity fields, leading to decadal-scale  
395 anomalous heat exchanges between the two basins<sup>21,96</sup>, and suggesting a potential oceanic  
396 pathway for the Indian Ocean influence on TPDV.

397  
398 The location of the winds that are most influential on the STC decadal variations is key to  
399 understanding their role in TPDV. The seminal results obtained with simplified ocean  
400 models<sup>75,78</sup> suggested that wind variations in the subtropical regions could control the STC  
401 transport and remotely affect equatorial SSTs. However, meridional transport changes at each  
402 latitude appear to be established by westward-propagating oceanic Rossby waves, as part of  
403 the tropical adjustment to varying winds, and be largely controlled by the local wind forcing<sup>18</sup>,  
404 although influences from the 15°-20° latitude band may also play a role at decadal  
405 timescales<sup>83,97-99</sup>. The possible origin and nature of these winds are discussed in the following  
406 sections.

407  
408



## 409 **Influences from Pacific extratropical atmospheric forcing**

410

411 Modes of internal atmospheric variability, such as the North Pacific Oscillation (NPO)<sup>100</sup> in  
412 the Northern Hemisphere and the South Pacific Oscillation (SPO)<sup>101</sup> in the Southern  
413 Hemisphere, extend toward the tropics, and can influence the tropical Pacific climate by  
414 changing the patterns of surface winds<sup>102,103</sup>. Subtropical/ tropical wind anomalies in the  
415 central-eastern Pacific alter the off-equatorial turbulent heat fluxes, resulting in SST anomalies  
416 that can persist for several months through the Wind-Evaporation-SST feedback<sup>104</sup> to impact  
417 equatorial dynamics. These SST patterns are known as the North and South Pacific Meridional  
418 Modes (NPMM and SPMM, respectively)<sup>105,106</sup>. The NPMM extends southwestward from the  
419 coast of California to the central equatorial Pacific<sup>106</sup> (Fig. 6a), while the SPMM exhibits SST  
420 anomalies along the South American coast, elongating toward the equator<sup>105</sup> (Fig. 6b). The  
421 processes by which the NPMM and SPMM can impact equatorial dynamics are clearer for the  
422 NPMM. They include the excitation of Summer deep convection near the ITCZ, which can  
423 result in equatorial wind anomalies<sup>107</sup>, and heat recharge/discharge in the equatorial pycnocline  
424 through meridional flows induced by NPMM-related wind stress curl anomalies, a process  
425 known as Tropical Wind Charging<sup>108</sup>. Both processes can affect ENSO development, but the  
426 Tropical Wind Charging mechanism appears to be the dominant player<sup>109,110</sup>.

427

428 While the Meridional Modes are well-known ENSO precursors<sup>103,105,107,111,112</sup>, they are also  
429 involved in the development of TPDV. This was first shown with atmospheric models coupled  
430 to slab ocean models, namely ocean models that provide ocean memory, but lack ocean  
431 dynamics<sup>113,114</sup>. In these “Atm-Slab” models, frequency spectrum reddening of weather and  
432 climate variability at decadal timescales appeared to occur through a sequence of extratropical-  
433 to-tropical influences (ENSO precursors to ENSO development) and tropical-to-extratropical  
434 feedbacks (ENSO teleconnections)<sup>113</sup> – a series of links supported by observational analyses<sup>115</sup>.  
435 Indeed, model experiments<sup>116</sup> indicate that ENSO teleconnections from the central equatorial  
436 Pacific can reinforce the NPMM and increase its persistence, resulting in the decadal NPMM  
437 variations detected in century-long coral time series from the northeastern subtropical  
438 Pacific<sup>117</sup>.

439

440 TPDV anomalies obtained in Atm-Slab models are weaker and centred further south than those  
441 obtained in fully coupled climate models and observations, highlighting the effect of oceanic  
442 processes<sup>45,114</sup>. Additionally, the tropical wind anomalies associated with the Meridional  
443 Modes can induce meridional pycnocline flow, as illustrated by the Tropical Wind Charging  
444 mechanism, and could therefore provide the atmospheric forcing needed to alter the strength  
445 of the STCs and produce equatorial SST anomalies, as previously discussed. Sensitivity  
446 experiments with simple dynamical models also indicate that extratropical stochastic wind  
447 forcing can produce low-frequency changes in the equatorial thermocline and multi-year ENSO  
448 variations<sup>118</sup>.

449

450 Since internal atmospheric variability typically peaks during the winter season in each  
451 hemisphere, they can independently influence the tropical Pacific. Some model results indicate  
452 a dominant influence of the Southern Hemisphere<sup>114,119-121</sup>. For example, a coupled model  
453 where the NPMM and SPMM were selectively disabled showed that the absence of the NPMM  
454 primarily impacted ENSO variability, while the SPMM significantly altered TPDV<sup>119</sup>. The  
455 prescription of heat fluxes typical of South Pacific Oscillation and North Pacific Oscillation  
456 forcing in century-long coupled model sensitivity experiments indicated a larger influence of  
457 the Southern Hemisphere on equatorial ocean dynamics responsible for TPDV<sup>121</sup>. Also,  
458 idealized coupled model experiments in which oceanic variability was nudged to climatological

459 values in the 30°S-10°S latitude band caused a ~30% reduction in decadal-scale SST variability  
460 in the equatorial Pacific<sup>120</sup>. The potential importance of the South Pacific influence has also  
461 emerged in an observational and modelling study<sup>122</sup>, which showed the important influence of  
462 South Pacific internal atmospheric variability on ENSO and Pacific decadal variability.

463  
464 On the other hand, a mode of variability linking the North Pacific with the Central Equatorial  
465 Pacific via the NPMM (and thus termed NP-CP mode) at decadal timescales has been recently  
466 identified in observations and ocean reanalyses<sup>31,38,123,124</sup> as a source of tropical Pacific decadal  
467 variance. This mode involves SST anomalies typical of the NPMM, and includes a SSH  
468 component with a pattern similar to that typical of decadal differences<sup>123</sup> (Fig. 1c), implying  
469 an important role for ocean dynamical processes.

470  
471 Thus, both hemispheres can potentially provide the atmospheric forcing for TPDV, but the  
472 question of which hemisphere dominates remains outstanding. The discrepancy between  
473 model- and observationally-based results regarding the influence of the North Pacific on TPDV  
474 likely reflects model deficiencies in capturing the North Pacific – Tropics interactions<sup>125</sup>, an  
475 aspect that warrants further investigation.

### 476 **Winds of Tropical Origin**

477  
478 Anomalous off-equatorial winds can also arise as a response to decadal SST anomalies<sup>116</sup>.  
479 Numerical simulations using an Atm-Slab model showed that SST anomalies prescribed in the  
480 central equatorial Pacific, where decadal anomalies are more prominent, can excite  
481 atmospheric Rossby waves, whose subtropical component may weaken the subtropical trade  
482 winds in both hemispheres<sup>116</sup> (Fig. 5a,b). Coupled climate model experiments with prescribed  
483 equatorial SST anomalies<sup>126</sup> yielded similar results. The equatorially-forced subtropical wind  
484 anomalies can then be expected to reinforce the equatorial anomaly through both  
485 thermodynamical processes, like Summer deep convection<sup>107</sup>, or changes in equatorward mass  
486 transport induced by the anomalous winds<sup>18</sup>, and create a feedback loop between equatorial  
487 and off-equatorial regions that can redden the spectra and contribute to the meridionally  
488 broader SST anomaly pattern found at decadal timescales<sup>4,14</sup>.

489  
490 Low-frequency equatorial SST anomalies can also alter the Walker and Hadley circulations. In  
491 particular, coupled model simulations with prescribed idealized warming along the Pacific  
492 equator, mimicking climate change conditions, show an intensification of the ascending branch  
493 of the Hadley circulation, and an enhancement of the off-equatorial trade winds. The ocean  
494 adjustment to these wind changes involves the spin-up of the STCs, leading to a cooling of the  
495 equatorial Pacific at some later time<sup>127</sup>. Changes in the strength of the Hadley Cells in response  
496 to equatorial decadal SST anomalies were also detected in other numerical simulations  
497 investigating the nature of Pacific decadal variability. These numerical experiments, conducted  
498 with different modelling frameworks, demonstrated that an anomalously warm tropical Pacific  
499 produces an increased poleward atmospheric energy transport<sup>128,129</sup>, and changes in off-  
500 equatorial Ekman pumping. The resulting ocean circulation adjustment leads to variations in  
501 STCs' strength and provides a delayed negative feedback to the original equatorial SST  
502 anomalies<sup>99,129</sup>. The opposite is found for cold decadal conditions in the tropical Pacific. These  
503 results suggest the possibility of a feedback loop between equatorial SST anomalies and off-  
504 equatorial wind variations which would support the view of TPDV as a tropical-extratropical  
505 coupled cyclic mode of variability. However, the ability to robustly detect these links in the  
506 relatively short observational record, given the presence of a large level of atmospheric noise  
507 remains a challenging scientific task that needs to be further explored in the future.  
508

509  
510  
511  
512  
513  
514  
515  
516  
517  
518  
519  
520  
521  
522  
523  
524  
525  
526  
527  
528  
529  
530  
531  
532  
533  
534  
535  
536  
537  
538  
539  
540  
541  
542  
543  
544  
545  
546  
547  
548  
549  
550  
551  
552  
553  
554  
555  
556  
557  
558

## **Influences from other oceans**

Outside all mechanisms internal to the Pacific basin that can influence TPDV, it has now been recognized that the Indian and Atlantic Oceans have the potential to generate variability in the Pacific<sup>130</sup>. Decadal SST variability in the Atlantic and Indian Oceans can generate inter-basin connections via changes in both atmospheric and oceanic circulations. The Indian to Pacific connections involve transport in the ITF (as previously discussed), while the ocean connection between the Atlantic and Pacific is considered small<sup>131</sup>. We thus focus on the atmospheric connections here.

Consider an SST anomaly in either the tropical Atlantic or Indian Ocean. The atmosphere responds with overlying anomalous atmospheric convection and diabatic heating, with accompanying near-surface zonal wind convergence into the convective region and a zonal wind divergence aloft (Fig. 5c, d). The diabatic heating generates an eastward-propagating equatorial Kelvin wave, and westward-propagating Rossby waves to the north and south of the heat source, inducing a descending motion throughout the rest of the tropics that is typically strongest where the Kelvin and Rossby waves meet (Fig. 5c, d). This so-called “Gill-type response”<sup>132</sup> alters the global Walker circulation on different timescales, from intra-seasonal through multidecadal<sup>133-140</sup>. These planetary waves act to spread the diabatically-generated tropospheric temperature anomaly through the entire tropics, a process commonly referred to as the “weak temperature gradient approximation”<sup>141,142</sup>. The resulting temperature changes away from the original heat source act to increase the vertical stability of the troposphere and reduce rainfall, a process known as the “tropospheric temperature mechanism”<sup>143</sup>. The two latter mechanisms provide thermodynamic explanations for the global Walker circulation changes (Fig. 5c, d). Alternate Atlantic to Pacific pathways have also been proposed to occur via the mid-latitudes along a curved pathway through the North Pacific to the western equatorial Pacific<sup>144,145</sup>; or through the tropics due to sea level pressure-induced surface wind changes across the Panama Isthmus<sup>146-148</sup>. Similarly, the linkages between the Indian to Pacific Ocean may also occur via wind changes across the Maritime Continent<sup>27</sup> or through stationary extratropical wave trains<sup>149</sup>.

Idealised numerical model experiments with prescribed surface warming in either the tropical Indian or Atlantic basins confirm the Gill-type induced global Walker circulation changes, including a Pacific trade wind acceleration (Fig. 5c,d), which leads to a central/eastern Pacific sea surface cooling in coupled model settings<sup>27,134,135,150-152</sup> and is further amplified by the Pacific Bjerknes feedback<sup>133,135,138</sup>. These Pacific changes on decadal timescales can also modulate ENSO characteristics<sup>151,153</sup>. While the inter-basin connections from the tropical Atlantic and Indian Oceans rely on broadly similar mechanisms, the location of the Atlantic SST forcing in relation to the Pacific implies that the resulting Rossby wave-induced wind anomalies also act to modulate eastern Pacific winds. Also, the descending motion response tends to be locally reinforced in the central Pacific where the Rossby and Kelvin waves collide (Fig. 5c, d).

TPDV appears to have responded to Atlantic and Indian Ocean forcing over the historical period. Using partially coupled experiments, where SSTs are constrained by idealised observed SST in one basin, Atlantic warming was shown to play a prominent role<sup>134,137,138,152</sup> in the transition from TPDV+ in the 1990s to TPDV- in the early 2000s<sup>11</sup>. The Indian Ocean was reported as either playing a minor role<sup>135,137</sup> or amplifying the Pacific response to the Atlantic forcing<sup>134</sup>. However, observations suggest that this recent dominance of the Atlantic may have

559 been different in the past<sup>130</sup>. The magnitude of the Pacific response to idealised Indian Ocean  
560 SST forcing appears to become more prominent further back in time (i.e., 1980-2010 or 1958-  
561 2010)<sup>140,149</sup>, while the response to Atlantic Ocean SST forcing appears relatively  
562 consistent<sup>130,144,152</sup>.

563

564 While there seems to be a reasonable understanding of this inter-basin connectivity, some  
565 questions remain regarding the exact mechanisms and their influence on TPDV. These include:  
566 What is the net effect of inter-basin coupling on TPDV amplitude? How has and will  
567 anthropogenic climate change alter these decadal inter-basin relationships<sup>154</sup>?

568

569 Other sources of uncertainties arise from the apparent discrepancies between some model  
570 results. For example, while inter-basin interactions are thought to amplify TPDV, model  
571 simulations in which the Atlantic or Indian Ocean influence is removed suggest instead that  
572 TPDV is intensified in the absence of Atlantic/Indian Ocean coupling<sup>155,156</sup>. Also, the  
573 connection between the Atlantic and Pacific becomes less clear when partially-coupled  
574 numerical experiments become more realistic<sup>157</sup>. These uncertainties indicate possible  
575 limitations of currently used partially-coupled experiments<sup>158</sup>, suggesting the need for  
576 additional research.

577

578

### 579 **Relative Importance of Different Mechanisms**

580

581 This Review has critically explored several mechanisms proposed to explain internal decadal  
582 variations in the tropical Pacific. While it is plausible that TPDV may simply arise as a residual  
583 of random ENSO variations<sup>4,32</sup>, modelling results indicate that TPDV leads decadal ENSO  
584 modulation by a few years<sup>45</sup>, suggesting that ENSO decadal changes are likely a consequence  
585 of the slowly varying background conditions, rather than causing them. However, the  
586 relationship between ENSO and TPDV is complex and warrants further investigation.

587

588 Results based on observations, ocean reanalyses, and models show a strong relationship  
589 between variations in the strength of the STCs at decadal timescales, as measured by the  
590 zonally-averaged equatorward pycnocline transport, and equatorial SSTAs, in support of the  
591  $v' \bar{T}$  hypothesis. However, the largest correlations occur at zero lag, making a causal  
592 relationship between STC transport and equatorial SST changes unlikely. Instead, these results  
593 suggest that the concurrent STC and equatorial SSTs variations are both part of the tropical  
594 pycnocline adjustment to varying wind forcing. This adjustment is mediated by Rossby wave  
595 activity, whose westward propagation alters the zonal slope of the pycnocline and produces  
596 meridional transport anomalies<sup>18</sup>. The adjustment timescale depends on the wave transit time,  
597 which increases with latitude, as well as the characteristics of the wind forcing relevant for  
598 TPDV.

599

600 Rossby wave activity alters pycnocline depth and manifests itself as temperature anomalies  
601 that propagate on mean isopycnals without a compensating salinity anomaly, thus  
602 encapsulating the non-compensated subset of the  $\bar{v}T'$  hypothesis. Apart from their transit times,  
603 these waves can also contribute to decadal timescales through their interaction with the forcing,  
604 for example by responding preferentially to the larger spatial and temporal scales of the  
605 winds<sup>71</sup>.

606

607 Propagation of salinity-compensated temperature anomalies (“spiciness anomalies”), another  
608 component of the  $\bar{v}T'$  hypothesis, is well supported by climate and ocean-only models<sup>55,61</sup>, but

609 the limited observational evidence available raises questions about whether these anomalies  
610 actually reach the equatorial region. In addition, an ocean-only model analysis suggests that  
611 the influence of spiciness anomalies on the heat budget of the equatorial thermocline may be  
612 small<sup>68</sup>.

613  
614 The origin of the atmospheric forcing driving the oceanic mechanisms at decadal time scales  
615 remains unclear. We have considered three main groups of atmospheric processes relevant for  
616 TPDV: The atmospheric response to decadal SSTAs in the equatorial Pacific; internal  
617 atmospheric variability in the extratropical Pacific; and atmospheric influences from the  
618 Atlantic and Indian Oceans. Current evidence suggests that these various processes may all be  
619 potentially important. Additional research is needed to more precisely assess their relative role  
620 in TPDV.

## 621 622 **Summary and Future Perspectives**

623  
624 Tropical Pacific decadal variations at periods between 7 and 70 years are linked to coherent  
625 basin-scale sea surface temperature and sea level pressure anomalies, and have global impacts.  
626 Despite a more limited historical record of subsurface data, it is clear that the surface  
627 manifestations of TPDV are associated with a reorganization of tropical Pacific upper-ocean  
628 heat content, most notably in the zonal direction, suggesting the involvement of ocean  
629 dynamical processes. Our Review has highlighted mechanisms of TPDV of which we are more  
630 confident, while pointing out aspects that are less certain and in need of additional research. In  
631 particular, the relationship between STC variability and changes in equatorial SSTs,  
632 underpinning the  $v'\bar{T}$  mechanism, emerges as a robust feature of TPDV across different  
633 datasets. The concurrent nature of this relationship does not support a causal influence of  
634 transport changes on SST changes, but instead highlights the importance of oceanic adjustment  
635 processes for modifying both quantities. This relationship holds for both interannual timescales  
636 associated with ENSO and for longer decadal timescales on which we have focused, suggesting  
637 that similar processes are operating on both timescales.

638  
639 In spite of these similarities with ENSO, questions remain about the nature of TPDV. While  
640 ENSO is an ocean-atmosphere coupled phenomenon, whose growth and phase transitions rely  
641 on coupled feedbacks, it is not clear if this is also true for TPDV. Although there are indications  
642 that low-frequency equatorial heating<sup>127</sup>, or individual ENSO events<sup>37</sup> can induce off-  
643 equatorial winds favourable for a TPDV phase reversal, there is still uncertainty about the  
644 origin and nature of the winds involved. Internally-generated wind anomalies in the  
645 subtropical/tropical regions can create equatorial SST anomalies<sup>102</sup>, which can then reinforce  
646 the subtropical wind anomalies through atmospheric teleconnections, increasing their  
647 persistence to enhance lower-frequency variability<sup>116</sup>. Decadal timescale SST anomalies in the  
648 Atlantic and Indian Oceans can also induce wind anomalies in the tropical Pacific conducive  
649 to the development of SST anomalies of the opposite sign<sup>134,137,150,152</sup>. However, the extent to  
650 which wind forcing from the extra-tropics or from other ocean basins may itself be the result  
651 of forcing from the tropical Pacific is not clearly understood. Furthermore, the relative  
652 magnitude of these various sources of wind variability in forcing TPDV is not known. A further  
653 uncertainty is related to whether the wind variations arise from deterministic processes  
654 operating on decadal timescales, or whether the decadal timescale processes that we observe  
655 in the Pacific are simply the result of stochastic white noise forcing that the ocean integrates  
656 through its inertia to produce a red noise spectral response. A full understanding of TPDV  
657 requires that we resolve these outstanding uncertainties via further research.

658

659 Properly designed coupled model sensitivity experiments, where SSTs are prescribed in certain  
660 regions could be used to isolate the contribution of the different regional sources of wind  
661 anomalies. Since these experiments may be affected by model biases and delicate to conduct<sup>158</sup>,  
662 they should be complemented by analyses of multi-variate empirical models<sup>159</sup>, which are  
663 trained on observations and allow a cleaner decoupling of feedbacks among different variables  
664 and regions<sup>160-162</sup>. In addition, simple ocean models that capture Rossby wave dynamics<sup>18,163</sup>  
665 can help assess the role of different aspects of the winds, including location and spectral  
666 characteristics, in reproducing key features of TPDV.

667

668 Although spiciness anomalies do not seem to significantly affect TPDV, current evidence is  
669 based on a limited number of analyses using just over two decades of observations available  
670 from the Argo floats, and primarily conducted with ocean-only models. However, the expected  
671 concentration of variance at decadal time scales of spiciness anomalies arriving at the equator,  
672 and the resulting rearrangement of the tropical climate, suggests that spiciness anomalies could  
673 still be potentially important driver of TPDV in the coupled setting. Thus, the role of spiciness  
674 should be further investigated in the context of coupled models. Availability of long time series  
675 from model simulations with realistic mixing parameterizations, achieved through either higher  
676 spatial resolution or improved model design, would be critical to more reliably assess the  
677 impact of spiciness on TPDV.

678

679 This review has focused on the oceanic and atmospheric processes that govern TPDV arising  
680 naturally within the climate system. We have not addressed the question of how TPDV may  
681 change in response to external forcing. However, we can expect changes in the characteristics  
682 of TPDV as a result of anthropogenic forcing. Increasing surface temperatures will result in  
683 increased ocean stratification<sup>164</sup>, leading to faster Rossby wave propagation, shorter adjustment  
684 timescales and reduced growth and predictability of Pacific decadal variability<sup>165</sup>, which may  
685 lead to weaker, shorter timescale TPDV in the future<sup>166</sup>. The expected reduced influence of  
686 Atlantic variability on ENSO, due to increased tropospheric stability<sup>167</sup> may also reduce the  
687 influence of Atlantic decadal variability on TPDV. On the other hand, the Wind Evaporation  
688 SST feedback is projected to increase due to warmer sea surface temperatures and increased  
689 evaporative response, which can lead to an enhanced impact of the NPM on ENSO and  
690 possibly on TPDV<sup>168,169</sup>. These and other possible processes, and their interactions, need to be  
691 assessed in climate models to determine how TPDV may change in a warmer world.

692

693

### 694 **Box 1. Mean ocean and atmospheric circulations in the tropical Pacific**

695

696 The equatorial Pacific Ocean is often described as a system with a warmer and dynamically  
697 active upper layer, and a colder and more quiescent bottom layer (shading along the equator,  
698 figure, bottom). These two layers are separated by a region of sharp vertical density  
699 (temperature) gradients, known as the pycnocline (thermocline), and are overlaid by a near-  
700 surface frictional layer – the Ekman layer.

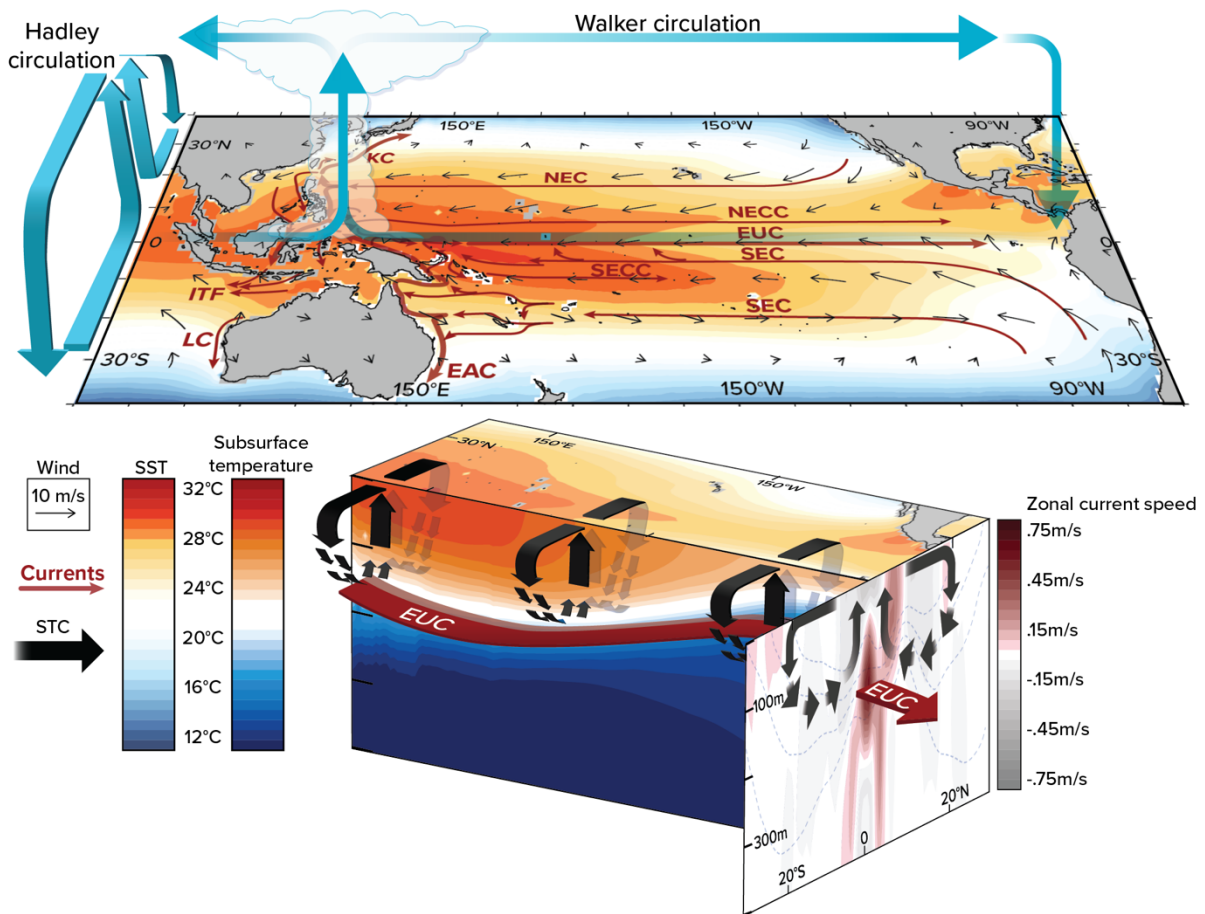
701

702 The pycnocline links subtropical regions to the equator: subtropical waters can penetrate into  
703 the ocean interior at the latitudes where surfaces of constant density (isopycnals) meet the near  
704 surface layer, and then flow equatorward along those isopycnals (black dashed lines in bottom  
705 panel of figure, Fig. 3 for a three-dimensional perspective). At the equator, these waters are  
706 brought to the upper layers by the upward vertical velocity (a process known as upwelling),  
707 and returned to higher latitudes by the flow in the surface Ekman layer (black solid arrows in  
708 bottom panel of figure), creating shallow overturning circulations in both hemispheres termed

709 Subtropical Cells (STCs)<sup>75</sup>. Warm tropical SSTs drive the atmospheric Hadley Cells (see  
 710 figure, top), with air rising near the equator, flowing poleward in the troposphere at 10-15 km  
 711 above the surface, and descending in the subtropics, with an equatorward return flow near the  
 712 surface that is deflected westward because of the Earth's rotation, creating the easterly trade  
 713 winds.  
 714

715 The tropical Pacific Ocean circulation also exhibits a rich system of zonal currents, (see figure,  
 716 top) with both westward and eastward flowing currents, the most noteworthy of which is the  
 717 Equatorial Undercurrent (EUC), a strong eastward flowing jet centred on the equator with a  
 718 core in the pycnocline (see figure, bottom). The zonal slope of the pycnocline - deeper in the  
 719 west, and shallower in the east - is in balance with the easterly equatorial trade winds, and  
 720 provides the pressure gradients that drives the EUC. The trade winds are the surface branch of  
 721 the zonal atmospheric Walker circulation, consisting of an ascending branch over the warm  
 722 waters of the western equatorial Pacific "Warm Pool", and a descending branch in the colder  
 723 and dryer eastern equatorial Pacific "Cold Tongue" (see figure, top).  
 724

725 The interior wind-driven zonal circulation is connected in the western Pacific to the  
 726 equatorward flowing Low-Latitude Western Boundary Currents (LLWBCs), which are an  
 727 important conduit for the redistribution of subtropical water to the western equatorial Pacific<sup>170</sup>  
 728 and then into the tropical current system, including the EUC and the Indonesian Throughflow  
 729 (ITF).  
 730



731  
 732  
 733 Box glossary  
 734

735 LLWBC: Low Latitude Western Boundary Current  
736 NEC: North Equatorial Current;  
737 NECC: North Equatorial Countercurrent;  
738 EUC: Equatorial Undercurrent;  
739 SEC: South Equatorial Current;  
740 SECC: South Equatorial Countercurrent;  
741 EAC: East Australian Current;  
742 ITF: Indonesian Throughflow;  
743 LC: Leeuwin Current;  
744 KC: Kuroshio Current

745  
746

## 747 **Box 2. Paleoclimate insights**

748

749 The brevity of the instrumental record limits analyses of TPDV with instrumental observations.  
750 Paleoclimate proxies, particularly tropical corals and sclerosponges, provide opportunities to  
751 track the low-frequency variations of the tropical oceans over centuries. Over the most recent  
752 phase transitions of TPDV, corals have recorded associated changes in dynamically relevant  
753 fields, including sea surface temperature<sup>171,172</sup>, salinity<sup>173-175</sup>, westerly wind bursts<sup>176</sup>, and  
754 upwelling<sup>177,178</sup>. Proxy records have provided evidence of interactions among different ocean  
755 basins at both interannual<sup>179</sup> and decadal<sup>180</sup> timescales. Proxy records from the Eastern Tropical  
756 North Pacific, where SST anomalies may reflect NPM activity, illustrate high levels of  
757 decadal variability coherent with the Central Equatorial Pacific records, supporting the  
758 potential involvement of the NPM in TPDV<sup>174</sup>.

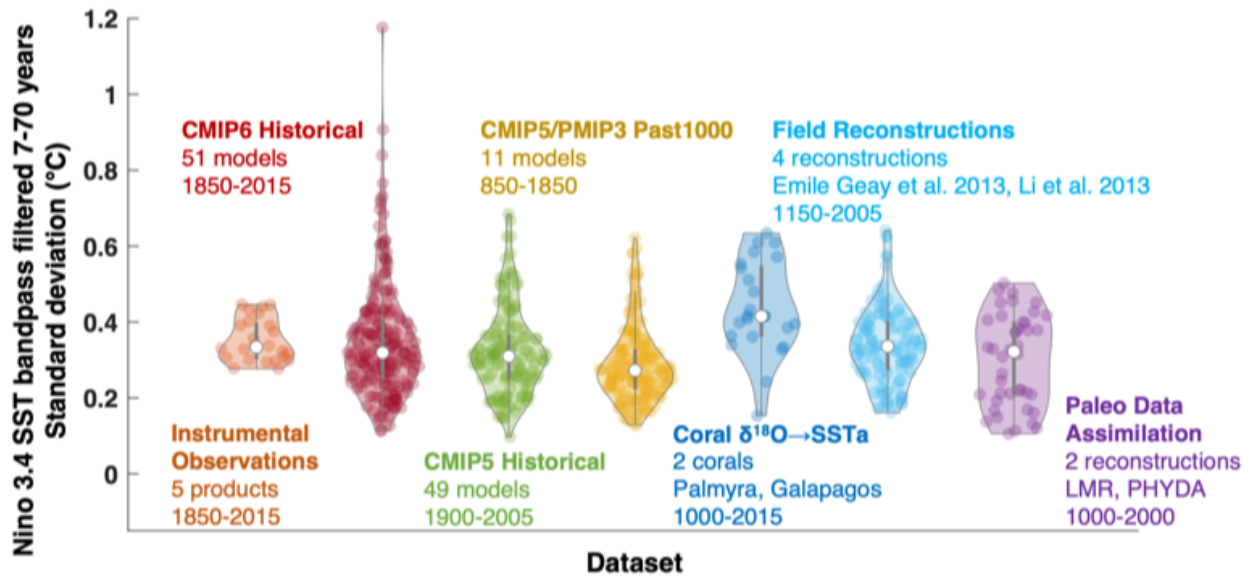
759

760 Additionally, paleoclimate analyses provide a perspective into the range of TPDV found over  
761 centuries-millennia, which can be used to assess model simulations of TPDV. The Box Figure  
762 compares TPDV across five different instrumental products, two generations of climate models  
763 (CMIP5, CMIP6; historical and Past1000 experiments), and three different sources of paleo  
764 data using violin plots<sup>181</sup>. TPDV is described in terms of the standard deviation of decadal  
765 variations (7-70 years) of the Niño3.4 index (annually average sea surface temperature  
766 anomalies in the 5°S-5°N, 170°W-120°W region). Violin plots for each dataset are based on  
767 decadal standard deviations of 100-year sliding windows allowing for 50 years overlap  
768 between segments. Individual dots represent the decadal standard deviation of each unique  
769 100-year segment. The median and interquartile range of these values is indicated by the white  
770 dots and vertical lines, respectively, while the width of the violin plot for each standard  
771 deviation indicates the corresponding frequency of occurrence. Notably, the instrumental  
772 record does not cover the full range of decadal variability suggested by both paleoclimate proxy  
773 reconstructions and climate models, although the median standard deviation is very similar  
774 among products.

775

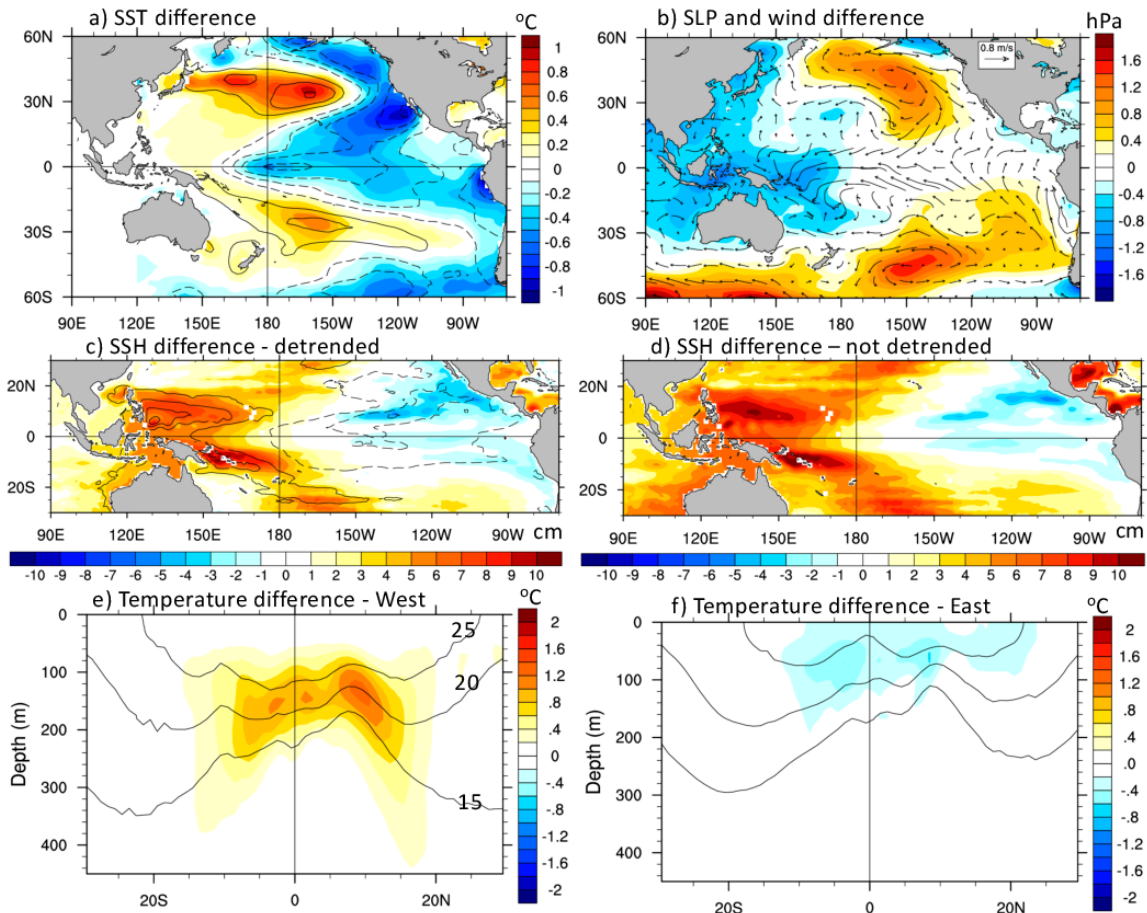
776



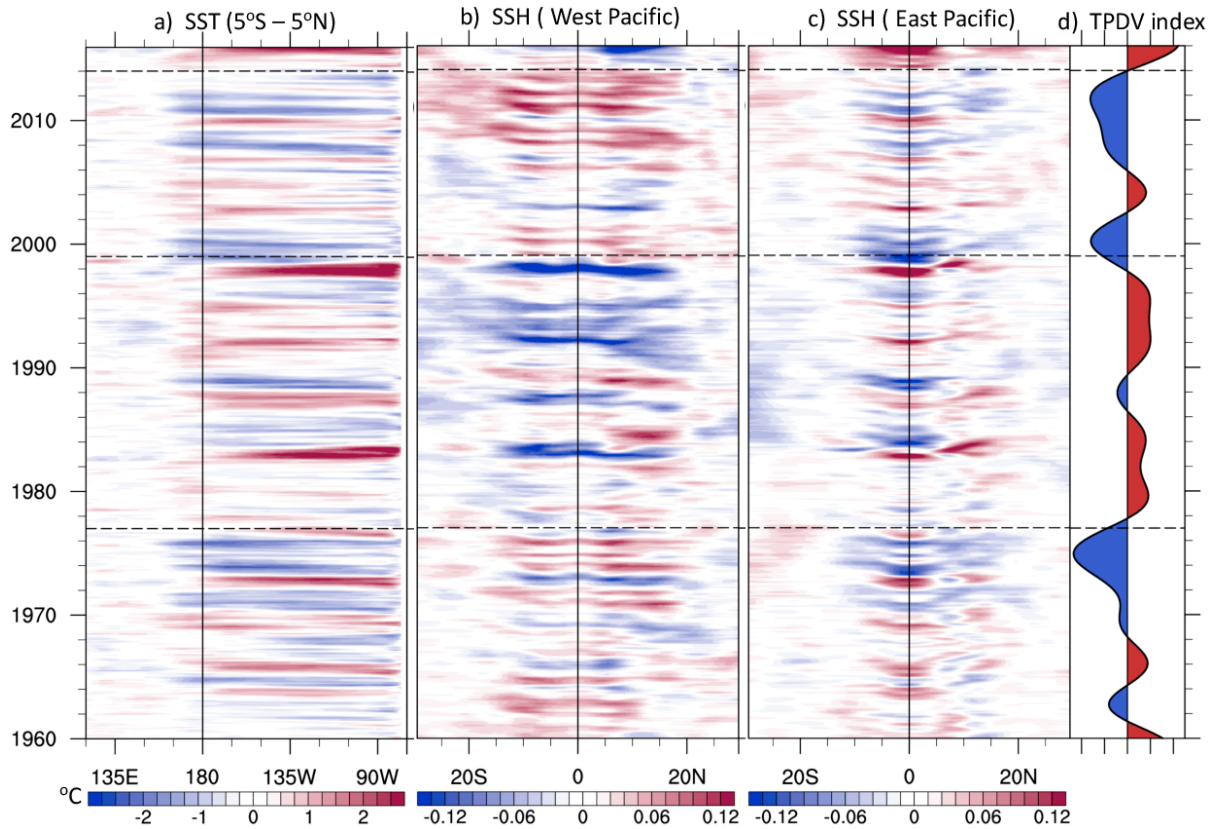


777  
778  
779  
780  
781  
782  
783  
784  
785  
786  
787  
788  
789  
790  
791  
792  
793  
794  
795  
796  
797  
798  
799  
800  
801  
802  
803  
804  
805  
806  
807  
808  
809  
810

811 **Figures**  
 812  
 813

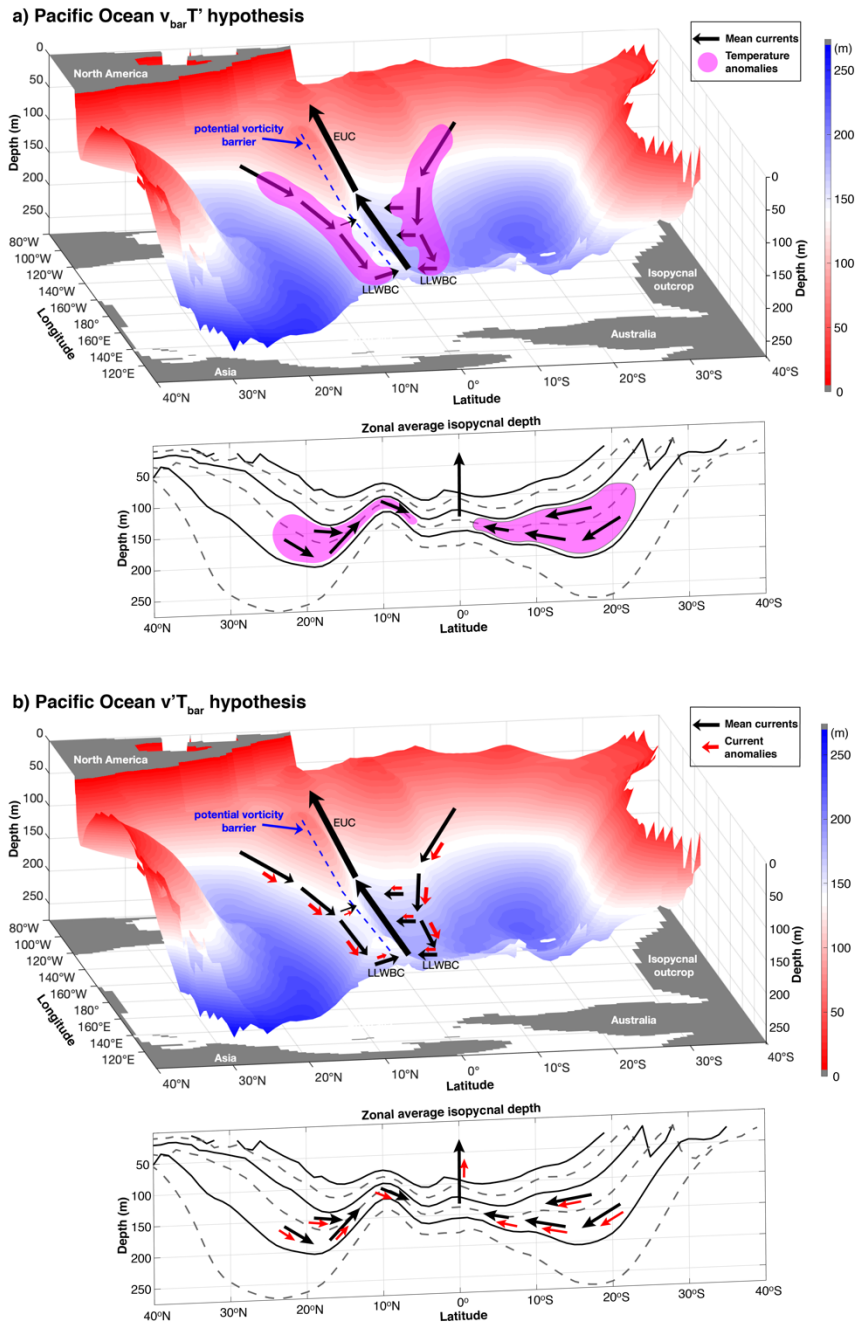


814 **Figure 1. Observed Pacific decadal changes.** a) The difference of linearly detrended SST anomalies<sup>182</sup>  
 815 between 1999-2014 (Period 2) (shading) and 1984-1999 (Period 1), and the negative phase of the basin-  
 816 wide TPDV pattern (contours). The TPDV pattern was obtained by regressing the decadal SST  
 817 anomalies on the TPDV index (leading Principal Component of decadal SST anomalies in 25°S-25°N).  
 818 b) Differences (Period 2 minus Period 1) of linearly detrended sea level pressure (shading) and vector  
 819 wind anomalies<sup>183</sup> (arrows) over 1958-2020 c) Differences of linearly detrended SSH anomalies<sup>184</sup>  
 820 (shading), and tropical SSH signature of TPDV, computed as the regression of decadal SSH anomalies  
 821 on the TPDV index. d) Same as c), but for un-detrended SSH data. e) Differences (Period 2 minus  
 822 Period 1) of detrended temperature anomalies zonally averaged between the western ocean boundary  
 823 and the dateline, and displayed as a function of latitude and depth. Contours indicate the time mean 15°,  
 824 20°, and 25° isotherms, highlighting the thermocline layer. f) Same as e), but for temperature values  
 825 averaged from the dateline to the eastern ocean boundary. SST contour interval in a) is 0.1°C, while  
 826 SSH contour interval in c) and d) is 1 cm. TPDV is associated with basin-wide SST, SLP and wind  
 827 anomalies, and involves a reorganization of heat content in the tropics.  
 828  
 829  
 830



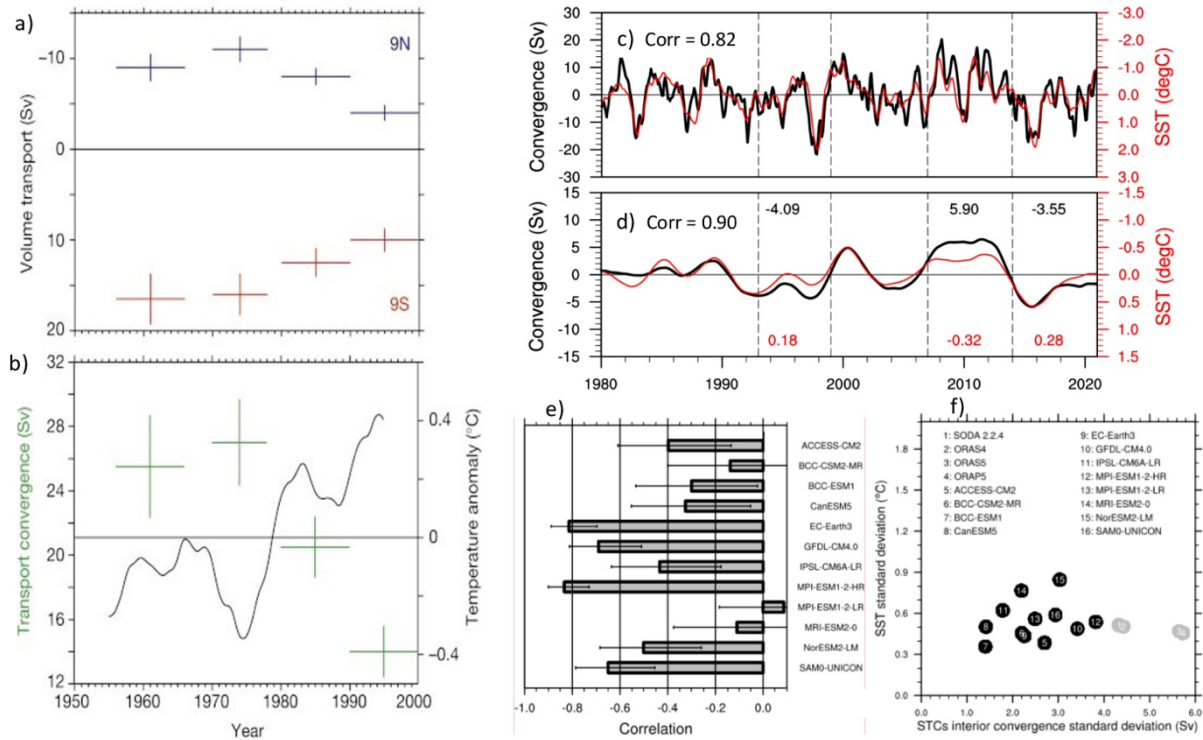
831  
 832  
 833  
 834  
 835  
 836  
 837  
 838  
 839  
 840  
 841  
 842  
 843  
 844

**Fig. 2. Relationship between TPDV and El Niño Southern Oscillation.** a) Evolution of SST anomalies<sup>182</sup> averaged in the equatorial band (5°S-5°N), displayed as a function of longitude (x-axis) and time (y-axis), with time increasing upward. b) Evolution of SSH anomalies<sup>185</sup> (m), a proxy for upper ocean heat content, averaged west of the dateline, as a function of latitude and time. c) Evolution of SSH anomalies (m) averaged east of the dateline, as a function of latitude and time. Anomalies of both SST and SSH are obtained by removing the climatological monthly mean and linearly detrending the data over the period 1958-2015. d) Time evolution of the TPDV index, computed as the leading Principal Component of decadal (7-70 years) SST anomalies in the tropical band (25°S-25°N). The index in d) is based on ERSSTv5. ENSO variability exhibits a decadal modulation with more El Niño activity and prevailing negative heat content anomalies in the western tropical Pacific during positive TPDV phases, and *vice versa* for negative TPDV phases.



846  
847  
848  
849  
850  
851  
852  
853  
854  
855  
856  
857  
858  
859

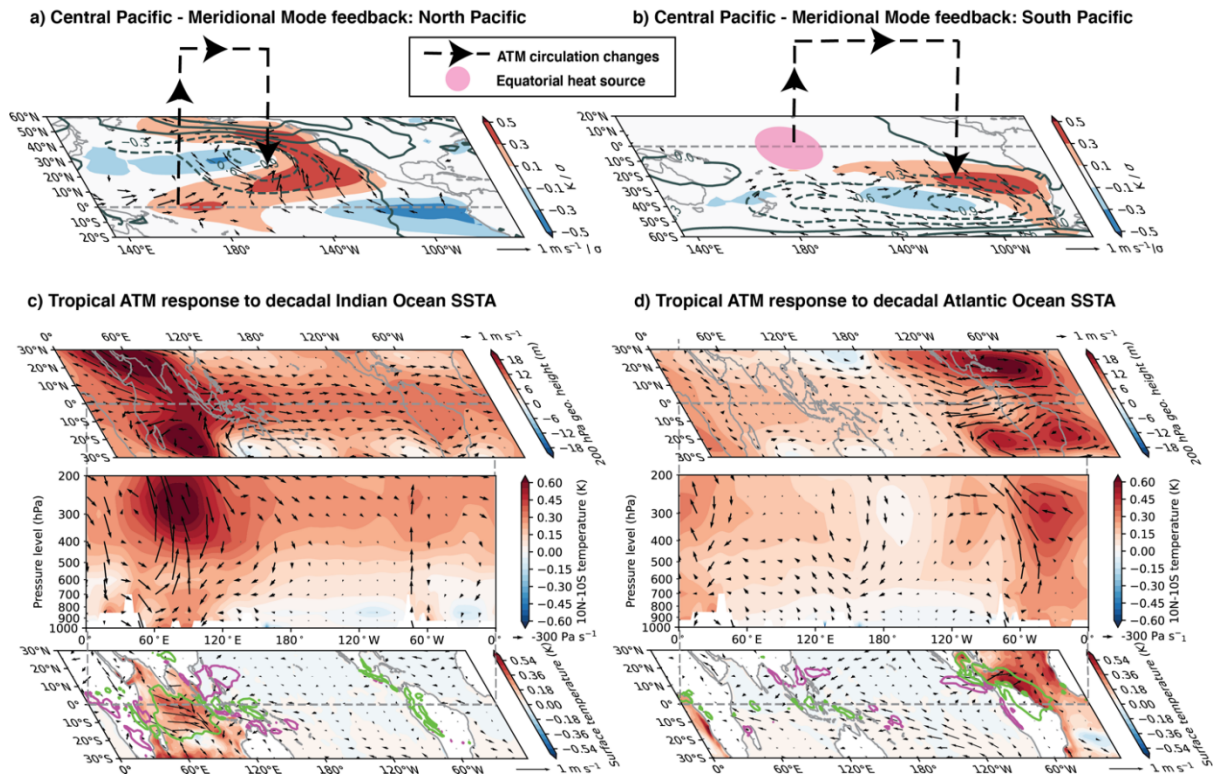
**Figure 3. Subtropical Cells influence on TPDV.** a) Schematic illustration of advection of spiciness anomalies (pink shading) by the mean circulation on the  $25.0 \text{ kg m}^{-3}$  isopycnal surface, illustrating the  $\bar{v}T'$  mechanism. Shading indicates isopycnal depth<sup>184</sup>. A density ridge in the  $5^{\circ}$ - $10^{\circ}$ N latitude band, known as “potential vorticity barrier”<sup>54</sup> is indicated by the gray dashed line. Equatorward spiciness flow along these isopycnal surfaces is also highlighted on the zonally averaged isopycnal depths (from  $23 \text{ kg m}^{-3}$  to  $25.5 \text{ kg m}^{-3}$  with a spacing of  $0.5 \text{ kg m}^{-3}$ ) in the latitude-depth plane on the bottom panel. b) Schematic illustration of the  $v'T$  mechanism, where the mean (black arrows) and anomalous (red arrows) flow are presented on the  $25.0 \text{ kg m}^{-3}$  isopycnal surface, which is located in the middle of the upper pycnocline. Flow along these isopycnal surfaces connects the subtropical to the tropical regions, as highlighted by the contours of zonally averaged isopycnal depth (from  $23 \text{ kg m}^{-3}$  to  $25.5 \text{ kg m}^{-3}$  with a spacing of  $0.5 \text{ kg m}^{-3}$ ) in the latitude-depth plane on the bottom panel. Both  $\bar{v}T'$  and  $v'T$  mechanisms were proposed as potential contributors to TPDV.



861  
862

863 **Figure 4. Assessment of the  $v'\bar{T}$  hypothesis.** a) Observational estimates of mean zonally-integrated  
 864 interior meridional pycnocline transports at 9°N and 9°S computed over 1956-65, 1970-77, 1980-89,  
 865 and 1990-99. Transport units are Sverdrups ( $1\text{Sv} = 10^6 \text{ m}^3 \text{ s}^{-1}$ ). Error bars are for one standard deviation  
 866 error. b) Mean meridional transport convergence (in Sv) across 9°N and 9°S computed as the difference  
 867 between Southern Hemisphere minus Northern Hemisphere transports. SST anomalies averaged over  
 868 the central and eastern equatorial Pacific (9°N-9°S, 90°W-180°W). c) Meridional transport convergence  
 869 anomalies (seasonal cycle removed) across 9.5°N and 9.5°S in the Pacific from the GODAS ocean  
 870 reanalysis<sup>186</sup> during 1980-2021. Transport convergence is compared with SST anomalies averaged over  
 871 9.5°N-9.5°S, 90°W-180°W. Meridional velocity anomalies used to compute the transports and SST  
 872 anomalies are linearly detrended. Correlation at zero lag between the time series is -0.82. d) Same as c)  
 873 but for 7-year low pass filtered anomalies. Correlation at zero lag is -0.90. Numerals in d) indicate  
 874 values of mean decadal transport anomalies (black) and mean decadal SST anomalies (red) over the  
 875 periods identified by the vertical dashed lines. e) Correlations between transport convergence at 9°N  
 876 and 9°S and equatorial SST anomalies in four ocean reanalyses<sup>184,185,187,188</sup> and 12 CMIP6 historical  
 877 simulations. For each model, the 95% confidence interval is shown. f) Standard deviation of equatorial  
 878 SST anomalies vs. the standard deviation of the transport convergence at 9°N and 9°S for the ocean  
 879 reanalyses and the historical CMIP6 simulations. Panels a) and b) are from <sup>19</sup>, panels c) and d) are  
 880 adapted from <sup>18</sup>, and panels e) and f) are adapted from <sup>88</sup>.

881



882  
883  
884  
885  
886  
887  
888  
889  
890  
891  
892  
893  
894  
895  
896  
897  
898  
899  
900  
901  
902  
903

**Figure 5. Atmospheric processes involved in TPDV.** a) SST (shading) and sea level pressure (SLP, contours) anomalies typical of the North Pacific Meridional Mode (NPMM). The SLP anomalies are associated with changes in the off-equatorial trade winds, which produce SST anomalies through the wind-evaporation-SST feedback. b) As in a), but for the South Pacific Meridional Mode (SPMM). To calculate these indices, we linearly remove the Niño 3.4 index influence on wind and SST anomalies<sup>106</sup> and identify the NPMM and SPMM indices, respectively, as the first SST expansion timeseries of an SST-wind maximum covariance analysis performed over 21°S-32°N, 175°E-95°W<sup>106</sup> and 10°S-35°S, 180°E-70°W<sup>189</sup>. The tropical atmospheric response to positive interdecadal SST differences in the Indian (1999-2008 minus 1988-1998) and Atlantic (1999-2014 minus 1982-1998) Oceans is respectively presented in c) and d). The lower panel includes the forcing SST anomalies in shading, while the modelled precipitation anomalies are shown as contours (green=positive; purple=negative), and the overlaying wind vectors represent the surface zonal and meridional winds. The mid-panels present equatorial sections of temperature (shading) and zonal and vertical wind vectors (arrows), meridionally averaged in the (10°S-10°N) latitude band. Note that the vertical winds are magnified by a factor of 300 to ensure scale comparability with the zonal wind. The upper panel represents the 200hPa geopotential height (shading) with overlaying wind vectors representing the 200hPa zonal and meridional winds. Data presented in c) and d) are based off AGCM simulations run by<sup>190</sup> and Naha et al. (2023b, in revision).

904 **Competing interests**

905

906 The authors declare no competing interests

907

908

909 **Acknowledgements**

910

911 This paper is a product of the CLIVAR Pacific Region Panel working group on “Tropical  
912 Pacific Decadal Variability”. The authors would like to thank CLIVAR for their sponsorship,  
913 and Ms. Jing Li at the CLIVAR Program Office for her help. The paper was finalized during a  
914 workshop held at Monash University, Australia. We acknowledge workshop funding support  
915 from the Faculty of Science and the School of Earth Atmosphere and Environment at Monash  
916 University, as well as CLIVAR and US CLIVAR. We also thank Natalie Renier from the  
917 Woods Hole Oceanographic Institution graphics team for her help in the preparation of Figure  
918 1. A.C. was supported by the NOAA Climate Program Office’s Climate Variability and  
919 Predictability (CVP) and Modeling, Analysis, Predictions, and Projections (MAPP) programs  
920 and by DOE Award #DE-SC0023228. S.M. was supported by the Australian Research Council  
921 (grant numbers FT160100162, DP200102329) and the Australian Government’s National  
922 Environmental Science Program (NESP2). M.F.S. was supported by NSF grant AGS-2141728  
923 and NOAA’s Climate Program Office’s Modeling, Analysis, Predictions, and Projections  
924 (MAPP) program grant NA20OAR4310445. This is IPRC publication X and SOEST  
925 contribution Y. Ag.S is supported by Australian Government’s National Environmental  
926 Science Program (NESP) and was supported by the Centre for Southern Hemisphere Oceans  
927 Research (CSHOR). K.B.K. was supported by the NASA Sea Level Change Science Program,  
928 Award 80NSSC20K1123. N.J.H. was supported by funding from the ARC Centre of  
929 Excellence for Climate Extremes (Grant No. CE170100023) and acknowledges support from  
930 the National Environmental Science Program (NESP) Climate Systems Hub. M.M. was  
931 supported by Austrian Science Fund project P33177. S.S. was supported by the U.S.  
932 Department of Energy, DE-SC0019418 and the US National Science Foundation, OCE-  
933 2202794 and AGS-1805143. C.M.V. was supported by Proyecto ANID Fondecyt 3200621.  
934 A.S.T. acknowledges the ARC Centre of Excellence for Climate Extremes and the Australian  
935 Government’s National Environmental Science Program (NESP). R.M.H. was supported by  
936 the Australian Research Council through grant DE21010004. C.C.U. was supported by NSF  
937 award AGS-2002083 and the *James E. and Barbara V. Moltz Fellowship for Climate-Related*  
938 *Research*. G.A.M. was supported by the Regional and Global Model Analysis (RGMA)  
939 component of the Earth and Environmental System Modelling Program of the U.S. Department  
940 of Energy's Office of Biological & Environmental Research (BER) under Award Number DE-  
941 SC0022070, and also by the National Center for Atmospheric Research, which is a major  
942 facility sponsored by the National Science Foundation (NSF) under Cooperative Agreement  
943 No. 1852977. N.S. acknowledges support from the joint JAMSTEC-IPRC Collaborative  
944 Research project JICore. This is PMEL contribution no. 5499.

945

946 **Author contributions**

947

948 A.C. and S.M. conceived the study. A.C., S.M., M.J.M., S.C., N.J.H., Y.I., S.C.S., J.S., M.F.S.,  
949 M.Z. coordinated the writing of the various sections. A.C., S.M., C.C.U. and S.C.S led the  
950 analyses and the preparation of the figures. All authors contributed to the discussion and  
951 interpretation of the material and assisted with the writing of the manuscript, led by A.C.

952

953 **Peer review information**

954 *Nature Reviews Earth & Environment* thanks [Referee#1 name], [Referee#2 name] and the  
955 other, anonymous, reviewer(s) for their contribution to the peer review of this work.

#### 956 **Publisher's note**

957 Springer Nature remains neutral with regard to jurisdictional claims in published maps and  
958 institutional affiliations.

959

#### 960 **References**

961

962 1 Lyu, K., Zhang, X., Church, J. A., Hu, J. & Yu, J.-Y. Distinguishing the Quasi-Decadal  
963 and Multidecadal Sea Level and Climate Variations in the Pacific: Implications for the  
964 ENSO-Like Low-Frequency Variability. *Journal of Climate* **30**, 5097-5117 (2017).  
965 [https://doi.org:https://doi.org/10.1175/JCLI-D-17-0004.1](https://doi.org/https://doi.org/10.1175/JCLI-D-17-0004.1)

966 2 Mantua, N. J., Hare, S. R., Zhang, Y., Wallace, J. M. & Francis, R. C. A Pacific  
967 Interdecadal Climate Oscillation with Impacts on Salmon Production\*. *Bulletin of the*  
968 *American Meteorological Society* **78**, 1069-1080 (1997).  
969 [https://doi.org:https://doi.org/10.1175/1520-](https://doi.org:https://doi.org/10.1175/1520-0477(1997)078<1069:APICOW>2.0.CO;2)  
970 [0477\(1997\)078<1069:APICOW>2.0.CO;2](https://doi.org:https://doi.org/10.1175/1520-0477(1997)078<1069:APICOW>2.0.CO;2)

971 3 Henley, B. J. *et al.* A Tripole Index for the Interdecadal Pacific Oscillation. *Climate*  
972 *Dynamics* **45**, 3077-3090 (2015). <https://doi.org:10.1007/s00382-015-2525-1>

973 4 Power, S. *et al.* Decadal climate variability in the tropical Pacific: Characteristics,  
974 causes, predictability, and prospects. *Science* **374**, eaay9165 (2021).  
975 <https://doi.org:doi:10.1126/science.aay9165>

976 5 Okumura, Y. M., Sun, T. & Wu, X. Asymmetric Modulation of El Niño and La Niña  
977 and the Linkage to Tropical Pacific Decadal Variability. *Journal of Climate* **30**, 4705-  
978 4733 (2017). <https://doi.org:https://doi.org/10.1175/JCLI-D-16-0680.1>

979 6 Capotondi, A., Deser, C., Phillips, A. S., Okumura, Y. & Larson, S. M. ENSO and  
980 Pacific Decadal Variability in the Community Earth System Model Version 2. *J Adv*  
981 *Model Earth Sy* **12**, e2019MS002022 (2020).  
982 <https://doi.org:https://doi.org/10.1029/2019MS002022>

983 7 Maher, N., Kay, J. E. & Capotondi, A. Modulation of ENSO teleconnections over North  
984 America by the Pacific decadal oscillation. *Environmental Research Letters* **17**, 114005  
985 (2022). <https://doi.org:10.1088/1748-9326/ac9327>

986 8 Li, X. *et al.* Tropical teleconnection impacts on Antarctic climate changes. *Nature*  
987 *Reviews Earth & Environment* **2**, 680-698 (2021). [https://doi.org:10.1038/s43017-021-](https://doi.org:10.1038/s43017-021-00204-5)  
988 [00204-5](https://doi.org:10.1038/s43017-021-00204-5)

989 9 Kosaka, Y. & Xie, S.-P. Recent global-warming hiatus tied to equatorial Pacific surface  
990 cooling. *Nature* **501**, 403-407 (2013). <https://doi.org:10.1038/nature12534>

991 10 Meehl, G. A., Hu, A., Santer, B. D. & Xie, S.-P. Contribution of the Interdecadal Pacific  
992 Oscillation to twentieth-century global surface temperature trends. *Nat Clim Change* **6**,  
993 1005-1008 (2016). <https://doi.org:10.1038/nclimate3107>



- 994 11 England, M. H. *et al.* Recent intensification of wind-driven circulation in the Pacific  
995 and the ongoing warming hiatus. *Nature Climate Change* **4**, 222-227 (2014).  
996 <https://doi.org:10.1038/nclimate2106>
- 997 12 Kociuba, G. & Power, S. B. Inability of CMIP5 Models to Simulate Recent  
998 Strengthening of the Walker Circulation: Implications for Projections. *Journal of*  
999 *Climate* **28**, 20-35 (2015). <https://doi.org:https://doi.org/10.1175/JCLI-D-13-00752.1>
- 1000 13 McGregor, S., Stuecker, M. F., Kajtar, J. B., England, M. H. & Collins, M. Model  
1001 tropical Atlantic biases underpin diminished Pacific decadal variability. *Nature Climate*  
1002 *Change* **8**, 493-498 (2018). <https://doi.org:10.1038/s41558-018-0163-4>
- 1003 14 Zhang, Y., Wallace, J. M. & Battisti, D. S. ENSO-like interdecadal variability: 1900-  
1004 93. *Journal of Climate* **10**, 1004-1020 (1997). [https://doi.org:Doi 10.1175/1520-0442\(1997\)010<1004:Eliv>2.0.Co;2](https://doi.org:Doi 10.1175/1520-0442(1997)010<1004:Eliv>2.0.Co;2)
- 1006 15 Qiu, B. & Chen, S. Multidecadal Sea Level and Gyre Circulation Variability in the  
1007 Northwestern Tropical Pacific Ocean. *Journal of Physical Oceanography* **42**, 193-206  
1008 (2012). <https://doi.org:https://doi.org/10.1175/JPO-D-11-061.1>
- 1009 16 Hu, S. *et al.* Multi-decadal trends in the tropical Pacific western boundary currents  
1010 retrieved from historical hydrological observations. *Science China Earth Sciences* **64**,  
1011 600-610 (2021). <https://doi.org:10.1007/s11430-020-9703-4>
- 1012 17 Maher, N., England, M. H., Gupta, A. S. & Spence, P. Role of Pacific trade winds in  
1013 driving ocean temperatures during the recent slowdown and projections under a wind  
1014 trend reversal. *Climate Dynamics* **51**, 321-336 (2018). <https://doi.org:10.1007/s00382-017-3923-3>
- 1016 18 Capotondi, A. & Qiu, B. Decadal Variability of the Pacific Shallow Overturning  
1017 Circulation and the Role of Local Wind Forcing. *Journal of Climate* **36**, 1001-1015  
1018 (2023). <https://doi.org:https://doi.org/10.1175/JCLI-D-22-0408.1>
- 1019 19 McPhaden, M. J. & Zhang, D. Slowdown of the meridional overturning circulation in  
1020 the upper Pacific Ocean. *Nature* **415**, 603-608 (2002). <https://doi.org:10.1038/415603a>
- 1021 20 Nieves, V., Willis, J. K. & Patzert, W. C. Recent hiatus caused by decadal shift in Indo-  
1022 Pacific heating. *Science* **349**, 532-535 (2015).  
1023 <https://doi.org:doi:10.1126/science.aaa4521>
- 1024 21 Lee, S.-K. *et al.* Pacific origin of the abrupt increase in Indian Ocean heat content during  
1025 the warming hiatus. *Nature Geoscience* **8**, 445-449 (2015).  
1026 <https://doi.org:10.1038/ngeo2438>
- 1027 22 Lee, T. & McPhaden, M. J. Decadal phase change in large-scale sea level and winds in  
1028 the Indo-Pacific region at the end of the 20th century. *Geophysical Research Letters* **35**  
1029 (2008). <https://doi.org:https://doi.org/10.1029/2007GL032419>
- 1030 23 Li, Y., Han, W., Hu, A., Meehl, G. A. & Wang, F. Multidecadal Changes of the Upper  
1031 Indian Ocean Heat Content during 1965–2016. *Journal of Climate* **31**, 7863-7884  
1032 (2018). <https://doi.org:https://doi.org/10.1175/JCLI-D-18-0116.1>

- 1033 24 Ummenhofer, C. C., Murty, S. A., Sprintall, J., Lee, T. & Abram, N. J. Heat and  
1034 freshwater changes in the Indian Ocean region. *Nature Reviews Earth & Environment*  
1035 **2**, 525-541 (2021). <https://doi.org:10.1038/s43017-021-00192-6>
- 1036 25 Merrifield, M. A. & Maltrud, M. E. Regional sea level trends due to a Pacific trade  
1037 wind intensification. *Geophysical Research Letters* **38** (2011).  
1038 <https://doi.org:https://doi.org/10.1029/2011GL049576>
- 1039 26 McGregor, S., Gupta, A. S. & England, M. H. Constraining Wind Stress Products with  
1040 Sea Surface Height Observations and Implications for Pacific Ocean Sea Level Trend  
1041 Attribution. *Journal of Climate* **25**, 8164-8176 (2012).  
1042 <https://doi.org:https://doi.org/10.1175/JCLI-D-12-00105.1>
- 1043 27 Han, W. *et al.* Intensification of decadal and multi-decadal sea level variability in the  
1044 western tropical Pacific during recent decades. *Climate Dynamics* **43**, 1357-1379  
1045 (2014). <https://doi.org:10.1007/s00382-013-1951-1>
- 1046 28 Weller, E. *et al.* Human-caused Indo-Pacific warm pool expansion. *Science Advances*  
1047 **2**, e1501719 (2016). <https://doi.org:doi:10.1126/sciadv.1501719>
- 1048 29 Hu, S. *et al.* Deep-reaching acceleration of global mean ocean circulation over the past  
1049 two decades. *Science Advances* **6**, eaax7727 (2020).  
1050 <https://doi.org:doi:10.1126/sciadv.aax7727>
- 1051 30 Luo, J.-J., Wang, G. & Dommenges, D. May common model biases reduce CMIP5's  
1052 ability to simulate the recent Pacific La Niña-like cooling? *Climate Dynamics* **50**, 1335-  
1053 1351 (2018). <https://doi.org:10.1007/s00382-017-3688-8>
- 1054 31 Newman, M. *et al.* The Pacific Decadal Oscillation, Revisited. *Journal of Climate* **29**,  
1055 4399-4427 (2016). <https://doi.org:10.1175/Jcli-D-15-0508.1>
- 1056 32 Vimont, D. J. The Contribution of the Interannual ENSO Cycle to the Spatial Pattern  
1057 of Decadal ENSO-Like Variability. *Journal of Climate* **18**, 2080-2092 (2005).  
1058 <https://doi.org:https://doi.org/10.1175/JCLI3365.1>
- 1059 33 Capotondi, A., Wittenberg, A. T., Kug, J.-S., Takahashi, K. & McPhaden, M. J. in *El*  
1060 *Niño Southern Oscillation in a Changing Climate* 65-86 (2020).
- 1061 34 McPhaden, M. J., Lee, T. & McClurg, D. El Niño and its relationship to changing  
1062 background conditions in the tropical Pacific Ocean. *Geophysical Research Letters* **38**  
1063 (2011). <https://doi.org:https://doi.org/10.1029/2011GL048275>
- 1064 35 McPhaden, M. J. Genesis and Evolution of the 1997-98 El Niño. *Science* **283**,  
1065 950-954 (1999). <https://doi.org:doi:10.1126/science.283.5404.950>
- 1066 36 Capotondi, A., Sardeshmukh, P. D. & Ricciardulli, L. The Nature of the Stochastic  
1067 Wind Forcing of ENSO. *Journal of Climate* **31**, 8081-8099 (2018).  
1068 <https://doi.org:https://doi.org/10.1175/JCLI-D-17-0842.1>
- 1069 37 Meehl, G. A., Teng, H., Capotondi, A. & Hu, A. The role of interannual ENSO events  
1070 in decadal timescale transitions of the Interdecadal Pacific Oscillation. *Climate*  
1071 *Dynamics* **57**, 1933-1951 (2021). <https://doi.org:10.1007/s00382-021-05784-y>

- 1072 38 Liu, C., Zhang, W., Jin, F.-F., Stuecker, M. F. & Geng, L. Equatorial Origin of the  
1073 Observed Tropical Pacific Quasi-Decadal Variability From ENSO Nonlinearity.  
1074 *Geophysical Research Letters* **49**, e2022GL097903 (2022).  
1075 [https://doi.org:https://doi.org/10.1029/2022GL097903](https://doi.org/https://doi.org/10.1029/2022GL097903)
- 1076 39 Gordon, E. M., Barnes, E. A. & Hurrell, J. W. Oceanic Harbingers of Pacific Decadal  
1077 Oscillation Predictability in CESM2 Detected by Neural Networks. *Geophysical*  
1078 *Research Letters* **48**, e2021GL095392 (2021).  
1079 <https://doi.org:https://doi.org/10.1029/2021GL095392>
- 1080 40 Capotondi, A. & Sardeshmukh, P. D. Is El Niño really changing? *Geophysical Research*  
1081 *Letters* **44**, 8548-8556 (2017). <https://doi.org:10.1002/2017gl074515>
- 1082 41 Fedorov, A. V. & Philander, S. G. Is El Niño Changing? *Science* **288**, 1997-2002  
1083 (2000). <https://doi.org:10.1126/science.288.5473.1997>
- 1084 42 Zhao, M., Hendon, H. H., Alves, O., Liu, G. & Wang, G. Weakened Eastern Pacific El  
1085 Niño Predictability in the Early Twenty-First Century. *Journal of Climate* **29**, 6805-  
1086 6822 (2016). <https://doi.org:https://doi.org/10.1175/JCLI-D-15-0876.1>
- 1087 43 Wang, G. & Hendon, H. H. Why 2015 was a strong El Niño and 2014 was not.  
1088 *Geophysical Research Letters* **44**, 8567-8575 (2017).  
1089 <https://doi.org:https://doi.org/10.1002/2017GL074244>
- 1090 44 Kim, G.-I. & Kug, J.-S. Tropical Pacific Decadal Variability Induced by Nonlinear  
1091 Rectification of El Niño–Southern Oscillation. *Journal of Climate* **33**, 7289-7302  
1092 (2020). <https://doi.org:https://doi.org/10.1175/JCLI-D-19-0123.1>
- 1093 45 Zhang, Y. *et al.* Role of ocean dynamics in equatorial Pacific decadal variability.  
1094 *Climate Dynamics* **59**, 2517-2529 (2022). <https://doi.org:10.1007/s00382-022-06312-2>
- 1095 46 Gu, D. & Philander, S. G. H. Interdecadal Climate Fluctuations That Depend on  
1096 Exchanges Between the Tropics and Extratropics. *Science* **275**, 805-807 (1997).  
1097 <https://doi.org:doi:10.1126/science.275.5301.805>
- 1098 47 Schneider, N., Miller, A. J., Alexander, M. A. & Deser, C. Subduction of Decadal North  
1099 Pacific Temperature Anomalies: Observations and Dynamics. *Journal of Physical*  
1100 *Oceanography* **29**, 1056-1070 (1999). [https://doi.org:https://doi.org/10.1175/1520-0485\(1999\)029<1056:SODNPT>2.0.CO;2](https://doi.org:https://doi.org/10.1175/1520-0485(1999)029<1056:SODNPT>2.0.CO;2)
- 1102 48 Luo, J.-J. & Yamagata, T. Long-term El Niño–Southern Oscillation (ENSO)-like  
1103 variation with special emphasis on the South Pacific. *Journal of Geophysical Research:*  
1104 *Oceans* **106**, 22211-22227 (2001).  
1105 <https://doi.org:https://doi.org/10.1029/2000JC000471>
- 1106 49 Luo, J.-J. *et al.* South Pacific origin of the decadal ENSO-like variation as simulated  
1107 by a coupled GCM. *Geophysical Research Letters* **30** (2003).  
1108 <https://doi.org:https://doi.org/10.1029/2003GL018649>
- 1109 50 Tatebe, H., Imada, Y., Mori, M., Kimoto, M. & Hasumi, H. Control of Decadal and  
1110 Bidecadal Climate Variability in the Tropical Pacific by the Off-Equatorial South

- 1111 Pacific Ocean. *Journal of Climate* **26**, 6524-6534 (2013).  
 1112 [https://doi.org:https://doi.org/10.1175/JCLI-D-12-00137.1](https://doi.org/https://doi.org/10.1175/JCLI-D-12-00137.1)
- 1113 51 Johnson, G. C. & McPhaden, M. J. Interior Pycnocline Flow from the Subtropical to  
 1114 the Equatorial Pacific Ocean. *Journal of Physical Oceanography* **29**, 3073-3089  
 1115 (1999). [https://doi.org:https://doi.org/10.1175/1520-  
 1116 0485\(1999\)029<3073:IPFFTS>2.0.CO;2](https://doi.org/https://doi.org/10.1175/1520-0485(1999)029<3073:IPFFTS>2.0.CO;2)
- 1117 52 Nonaka, M. & Xie, S.-P. Propagation of North Pacific interdecadal subsurface  
 1118 temperature anomalies in an ocean GCM. *Geophysical Research Letters* **27**, 3747-3750  
 1119 (2000). [https://doi.org:https://doi.org/10.1029/2000GL011488](https://doi.org/https://doi.org/10.1029/2000GL011488)
- 1120 53 Zeller, M., McGregor, S. & Spence, P. Hemispheric Asymmetry of the Pacific Shallow  
 1121 Meridional Overturning Circulation. *Journal of Geophysical Research: Oceans* **124**,  
 1122 5765-5786 (2019). [https://doi.org:https://doi.org/10.1029/2018JC014840](https://doi.org/https://doi.org/10.1029/2018JC014840)
- 1123 54 Lu, P. & McCreary, J. P. Influence of the ITCZ on the Flow of Thermocline Water from  
 1124 the Subtropical to the Equatorial Pacific Ocean. *Journal of Physical Oceanography* **25**,  
 1125 3076-3088 (1995). [https://doi.org:https://doi.org/10.1175/1520-  
 1126 0485\(1995\)025<3076:IOTIOT>2.0.CO;2](https://doi.org/https://doi.org/10.1175/1520-0485(1995)025<3076:IOTIOT>2.0.CO;2)
- 1127 55 Zeller, M., McGregor, S., van Sebille, E., Capotondi, A. & Spence, P. Subtropical-  
 1128 tropical pathways of spiciness anomalies and their impact on equatorial Pacific  
 1129 temperature. *Climate Dynamics* **56**, 1131-1144 (2021). [https://doi.org:10.1007/s00382-  
 1130 020-05524-8](https://doi.org/10.1007/s00382-020-05524-8)
- 1131 56 Munk, W. Internal waves and small scale processes. *Evolution of Physical  
 1132 Oceanography*, B. A. Warren and C. Wunsch, Eds., MIT Press, 264–291 (1981).
- 1133 57 Schneider, N. A decadal spiciness mode in the tropics. *Geophysical Research Letters*  
 1134 **27**, 257-260 (2000). [https://doi.org:https://doi.org/10.1029/1999GL002348](https://doi.org/https://doi.org/10.1029/1999GL002348)
- 1135 58 Yeager, S. G. & Large, W. G. Late-Winter Generation of Spiciness on Subducted  
 1136 Isopycnals. *Journal of Physical Oceanography* **34**, 1528-1547 (2004).  
 1137 [https://doi.org:https://doi.org/10.1175/1520-  
 1138 0485\(2004\)034<1528:LGOSOS>2.0.CO;2](https://doi.org/https://doi.org/10.1175/1520-0485(2004)034<1528:LGOSOS>2.0.CO;2)
- 1139 59 Yeager, S. G. & Large, W. G. Observational Evidence of Winter Spice Injection.  
 1140 *Journal of Physical Oceanography* **37**, 2895-2919 (2007).  
 1141 [https://doi.org:https://doi.org/10.1175/2007JPO3629.1](https://doi.org/https://doi.org/10.1175/2007JPO3629.1)
- 1142 60 Kilpatrick, T., Schneider, N. & Di Lorenzo, E. Generation of Low-Frequency Spiciness  
 1143 Variability in the Thermocline. *Journal of Physical Oceanography* **41**, 365-377 (2011).  
 1144 [https://doi.org:https://doi.org/10.1175/2010JPO4443.1](https://doi.org/https://doi.org/10.1175/2010JPO4443.1)
- 1145 61 Schneider, N. The Response of Tropical Climate to the Equatorial Emergence of  
 1146 Spiciness Anomalies. *Journal of Climate* **17**, 1083-1095 (2004).  
 1147 [https://doi.org:https://doi.org/10.1175/1520-  
 1148 0442\(2004\)017<1083:TROTCT>2.0.CO;2](https://doi.org/https://doi.org/10.1175/1520-0442(2004)017<1083:TROTCT>2.0.CO;2)

- 1149 62 Li, Y., Wang, F. & Sun, Y. Low-frequency spiciness variations in the tropical Pacific  
1150 Ocean observed during 2003–2012. *Geophysical Research Letters* **39** (2012).  
1151 [https://doi.org:https://doi.org/10.1029/2012GL053971](https://doi.org/https://doi.org/10.1029/2012GL053971)
- 1152 63 Katsura, S., Oka, E., Qiu, B. & Schneider, N. Formation and Subduction of North  
1153 Pacific Tropical Water and Their Interannual Variability. *Journal of Physical*  
1154 *Oceanography* **43**, 2400-2415 (2013). [https://doi.org:https://doi.org/10.1175/JPO-D-](https://doi.org:https://doi.org/10.1175/JPO-D-13-031.1)  
1155 [13-031.1](https://doi.org:https://doi.org/10.1175/JPO-D-13-031.1)
- 1156 64 Wang, T., Suga, T. & Kouketsu, S. Spiciness anomalies in the upper North Pacific  
1157 based on Argo observations. *Frontiers in Marine Science* **9** (2022).  
1158 <https://doi.org:10.3389/fmars.2022.1006042>
- 1159 65 Kolodziejczyk, N. & Gaillard, F. Observation of spiciness interannual variability in the  
1160 Pacific pycnocline. *Journal of Geophysical Research: Oceans* **117** (2012).  
1161 <https://doi.org:https://doi.org/10.1029/2012JC008365>
- 1162 66 Hu, S. *et al.* Observed Triple Mode of Salinity Variability in the Thermocline of  
1163 Tropical Pacific Ocean. *Journal of Geophysical Research: Oceans* **125**,  
1164 e2020JC016210 (2020). <https://doi.org:https://doi.org/10.1029/2020JC016210>
- 1165 67 Sasaki, Y. N., Schneider, N., Maximenko, N. & Lebedev, K. Observational evidence  
1166 for propagation of decadal spiciness anomalies in the North Pacific. *Geophysical*  
1167 *Research Letters* **37** (2010). <https://doi.org:https://doi.org/10.1029/2010GL042716>
- 1168 68 Zeller, M. *The Impact of Subtropical to Tropical Oceanic Interactions on Tropical*  
1169 *Pacific Decadal Variability*, Monash University, (2020).
- 1170 69 Albery, M. S. *et al.* Spatial patterns of mixing in the Solomon Sea. *Journal of*  
1171 *Geophysical Research: Oceans* **122**, 4021-4039 (2017).  
1172 <https://doi.org:https://doi.org/10.1002/2016JC012666>
- 1173 70 Capotondi, A. & Alexander, M. A. Rossby Waves in the Tropical North Pacific and  
1174 Their Role in Decadal Thermocline Variability. *Journal of Physical Oceanography* **31**,  
1175 3496-3515 (2001). [https://doi.org:https://doi.org/10.1175/1520-](https://doi.org:https://doi.org/10.1175/1520-0485(2002)031<3496:RWITTN>2.0.CO;2)  
1176 [0485\(2002\)031<3496:RWITTN>2.0.CO;2](https://doi.org:https://doi.org/10.1175/1520-0485(2002)031<3496:RWITTN>2.0.CO;2)
- 1177 71 Capotondi, A., Alexander, M. A. & Deser, C. Why Are There Rossby Wave Maxima  
1178 in the Pacific at 10°S and 13°N? *Journal of Physical Oceanography* **33**, 1549-1563  
1179 (2003). <https://doi.org:https://doi.org/10.1175/2407.1>
- 1180 72 Galanti, E. & Tziperman, E. A Midlatitude–ENSO Teleconnection Mechanism via  
1181 Baroclinically Unstable Long Rossby Waves. *Journal of Physical Oceanography* **33**,  
1182 1877-1888 (2003). [https://doi.org:https://doi.org/10.1175/1520-](https://doi.org:https://doi.org/10.1175/1520-0485(2003)033<1877:AMTMVB>2.0.CO;2)  
1183 [0485\(2003\)033<1877:AMTMVB>2.0.CO;2](https://doi.org:https://doi.org/10.1175/1520-0485(2003)033<1877:AMTMVB>2.0.CO;2)
- 1184 73 Imada, Y., Tatebe, H., Watanabe, M., Ishii, M. & Kimoto, M. South Pacific influence  
1185 on the termination of El Niño in 2014. *Scientific Reports* **6**, 30341 (2016).  
1186 <https://doi.org:10.1038/srep30341>
- 1187 74 McPhaden, M. J. Playing hide and seek with El Niño. *Nature Climate Change* **5**, 791-  
1188 795 (2015). <https://doi.org:10.1038/nclimate2775>

- 1189 75 McCreary, J. P. & Lu, P. Interaction between the Subtropical and Equatorial Ocean  
1190 Circulations: The Subtropical Cell. *Journal of Physical Oceanography* **24**, 466-497  
1191 (1994). [https://doi.org:https://doi.org/10.1175/1520-  
1192 0485\(1994\)024<0466:IBTSAE>2.0.CO;2](https://doi.org/https://doi.org/10.1175/1520-0485(1994)024<0466:IBTSAE>2.0.CO;2)
- 1193 76 Kleeman, R., McCreary Jr., J. P. & Klinger, B. A. A mechanism for generating ENSO  
1194 decadal variability. *Geophysical Research Letters* **26**, 1743-1746 (1999).  
1195 <https://doi.org:https://doi.org/10.1029/1999GL900352>
- 1196 77 Klinger, B. A., McCreary, J. P. & Kleeman, R. The Relationship between Oscillating  
1197 Subtropical Wind Stress and Equatorial Temperature. *Journal of Physical  
1198 Oceanography* **32**, 1507-1521 (2002). [https://doi.org:https://doi.org/10.1175/1520-  
1199 0485\(2002\)032<1507:TRBOSW>2.0.CO;2](https://doi.org:https://doi.org/10.1175/1520-0485(2002)032<1507:TRBOSW>2.0.CO;2)
- 1200 78 Solomon, A., McCreary, J. P., Kleeman, R. & Klinger, B. A. Interannual and Decadal  
1201 Variability in an Intermediate Coupled Model of the Pacific Region. *Journal of Climate*  
1202 **16**, 383-405 (2003). [https://doi.org:https://doi.org/10.1175/1520-  
1203 0442\(2003\)016<0383:IADVIA>2.0.CO;2](https://doi.org:https://doi.org/10.1175/1520-0442(2003)016<0383:IADVIA>2.0.CO;2)
- 1204 79 McPhaden, M. J. & Zhang, D. Pacific Ocean circulation rebounds. *Geophysical  
1205 Research Letters* **31** (2004). <https://doi.org:https://doi.org/10.1029/2004GL020727>
- 1206 80 Capotondi, A., Alexander, M. A., Deser, C. & McPhaden, M. J. Anatomy and Decadal  
1207 Evolution of the Pacific Subtropical–Tropical Cells (STCs). *Journal of Climate* **18**,  
1208 3739-3758 (2005). <https://doi.org:https://doi.org/10.1175/JCLI3496.1>
- 1209 81 Cheng, W., McPhaden, M. J., Zhang, D. & Metzger, E. J. Recent Changes in the Pacific  
1210 Subtropical Cells Inferred from an Eddy-Resolving Ocean Circulation Model. *Journal  
1211 of Physical Oceanography* **37**, 1340-1356 (2007).  
1212 <https://doi.org:https://doi.org/10.1175/JPO3051.1>
- 1213 82 Lübbecke, J. F., Böning, C. W. & Biastoch, A. Variability in the subtropical-tropical  
1214 cells and its effect on near-surface temperature of the equatorial Pacific: a model study.  
1215 *Ocean Sci.* **4**, 73-88 (2008). <https://doi.org:10.5194/os-4-73-2008>
- 1216 83 Farneti, R., Dwivedi, S., Kucharski, F., Molteni, F. & Griffies, S. M. On Pacific  
1217 Subtropical Cell Variability over the Second Half of the Twentieth Century. *Journal of  
1218 Climate* **27**, 7102-7112 (2014). [https://doi.org:https://doi.org/10.1175/JCLI-D-13-  
1219 00707.1](https://doi.org:https://doi.org/10.1175/JCLI-D-13-00707.1)
- 1220 84 Schott, F. A., Stramma, L., Wang, W., Giese, B. S. & Zantopp, R. Pacific Subtropical  
1221 Cell variability in the SODA 2.0.2/3 assimilation. *Geophysical Research Letters* **35**  
1222 (2008). <https://doi.org:https://doi.org/10.1029/2008GL033757>
- 1223 85 Jin, F.-F. An Equatorial Ocean Recharge Paradigm for ENSO. Part I: Conceptual  
1224 Model. *Journal of the Atmospheric Sciences* **54**, 811-829 (1997).  
1225 [https://doi.org:https://doi.org/10.1175/1520-  
1226 0469\(1997\)054<0811:AEORPF>2.0.CO;2](https://doi.org:https://doi.org/10.1175/1520-0469(1997)054<0811:AEORPF>2.0.CO;2)
- 1227 86 Wang, X., Jin, F.-F. & Wang, Y. A Tropical Ocean Recharge Mechanism for Climate  
1228 Variability. Part II: A Unified Theory for Decadal and ENSO Modes. *Journal of*

- 1229 *Climate* **16**, 3599-3616 (2003). [https://doi.org:https://doi.org/10.1175/1520-0442\(2003\)016<3599:ATORMF>2.0.CO;2](https://doi.org/10.1175/1520-0442(2003)016<3599:ATORMF>2.0.CO;2)  
1230
- 1231 87 Zhang, D. & McPhaden, M. J. Decadal variability of the shallow Pacific meridional  
1232 overturning circulation: Relation to tropical sea surface temperatures in observations  
1233 and climate change models. *Ocean Modelling* **15**, 250-273 (2006).  
1234 [https://doi.org:https://doi.org/10.1016/j.ocemod.2005.12.005](https://doi.org/10.1016/j.ocemod.2005.12.005)
- 1235 88 Graffino, G., Farneti, R. & Kucharski, F. Low-frequency variability of the Pacific  
1236 Subtropical Cells as reproduced by coupled models and ocean reanalyses. *Climate*  
1237 *Dynamics* **56**, 3231-3254 (2021). [https://doi.org:10.1007/s00382-021-05639-6](https://doi.org/10.1007/s00382-021-05639-6)
- 1238 89 Lee, T. & Fukumori, I. Interannual-to-Decadal Variations of Tropical–Subtropical  
1239 Exchange in the Pacific Ocean: Boundary versus Interior Pycnocline Transports.  
1240 *Journal of Climate* **16**, 4022-4042 (2003). [https://doi.org:https://doi.org/10.1175/1520-0442\(2003\)016<4022:IVOTEI>2.0.CO;2](https://doi.org/10.1175/1520-0442(2003)016<4022:IVOTEI>2.0.CO;2)  
1241
- 1242 90 Zilberman, N. V., Roemmich, D. H. & Gille, S. T. The Mean and the Time Variability  
1243 of the Shallow Meridional Overturning Circulation in the Tropical South Pacific Ocean.  
1244 *Journal of Climate* **26**, 4069-4087 (2013). [https://doi.org:https://doi.org/10.1175/JCLI-D-12-00120.1](https://doi.org/10.1175/JCLI-D-12-00120.1)  
1245
- 1246 91 Kessler, W. S., Hristova, H. G. & Davis, R. E. Equatorward western boundary transport  
1247 from the South Pacific: Glider observations, dynamics and consequences. *Progress in*  
1248 *Oceanography* **175**, 208-225 (2019).  
1249 [https://doi.org:https://doi.org/10.1016/j.pocean.2019.04.005](https://doi.org/10.1016/j.pocean.2019.04.005)
- 1250 92 Mayer, M., Haimberger, L. & Balmaseda, M. A. On the Energy Exchange between  
1251 Tropical Ocean Basins Related to ENSO. *Journal of Climate* **27**, 6393-6403 (2014).  
1252 [https://doi.org:https://doi.org/10.1175/JCLI-D-14-00123.1](https://doi.org/10.1175/JCLI-D-14-00123.1)
- 1253 93 Mayer, M., Alonso Balmaseda, M. & Haimberger, L. Unprecedented 2015/2016 Indo-  
1254 Pacific Heat Transfer Speeds Up Tropical Pacific Heat Recharge. *Geophysical*  
1255 *Research Letters* **45**, 3274-3284 (2018).  
1256 [https://doi.org:https://doi.org/10.1002/2018GL077106](https://doi.org/10.1002/2018GL077106)
- 1257 94 Mayer, M. & Balmaseda, M. A. Indian Ocean impact on ENSO evolution 2014–2016  
1258 in a set of seasonal forecasting experiments. *Climate Dynamics* **56**, 2631-2649 (2021).  
1259 [https://doi.org:10.1007/s00382-020-05607-6](https://doi.org/10.1007/s00382-020-05607-6)
- 1260 95 Hu, S. & Sprintall, J. Observed strengthening of interbasin exchange via the Indonesian  
1261 seas due to rainfall intensification. *Geophysical Research Letters* **44**, 1448-1456  
1262 (2017). [https://doi.org:https://doi.org/10.1002/2016GL072494](https://doi.org/10.1002/2016GL072494)
- 1263 96 Ummenhofer, C. C., Biastoch, A. & Böning, C. W. Multidecadal Indian Ocean  
1264 Variability Linked to the Pacific and Implications for Preconditioning Indian Ocean  
1265 Dipole Events. *Journal of Climate* **30**, 1739-1751 (2017).  
1266 [https://doi.org:https://doi.org/10.1175/JCLI-D-16-0200.1](https://doi.org/10.1175/JCLI-D-16-0200.1)
- 1267 97 Nonaka, M., Xie, S.-P. & McCreary, J. P. Decadal variations in the subtropical cells  
1268 and equatorial pacific SST. *Geophysical Research Letters* **29**, 20-21-20-24 (2002).  
1269 [https://doi.org:https://doi.org/10.1029/2001GL013717](https://doi.org/10.1029/2001GL013717)

- 1270 98 Graffino, G., Farneti, R., Kucharski, F. & Molteni, F. The Effect of Wind Stress  
1271 Anomalies and Location in Driving Pacific Subtropical Cells and Tropical Climate.  
1272 *Journal of Climate* **32**, 1641-1660 (2019). [https://doi.org/10.1175/JCLI-](https://doi.org/10.1175/JCLI-D-18-0071.1)  
1273 [D-18-0071.1](https://doi.org/10.1175/JCLI-D-18-0071.1)
- 1274 99 Meehl, G. A. & Hu, A. Megadroughts in the Indian Monsoon Region and Southwest  
1275 North America and a Mechanism for Associated Multidecadal Pacific Sea Surface  
1276 Temperature Anomalies. *Journal of Climate* **19**, 1605-1623 (2006).  
1277 <https://doi.org/10.1175/JCLI3675.1>
- 1278 100 Rogers, J. C. The North Pacific Oscillation. *Journal of Climatology* **1**, 39-57 (1981).  
1279 <https://doi.org/10.1002/joc.3370010106>
- 1280 101 You, Y. & Furtado, J. C. The role of South Pacific atmospheric variability in the  
1281 development of different types of ENSO. *Geophysical Research Letters* **44**, 7438-7446  
1282 (2017). <https://doi.org/10.1002/2017GL073475>
- 1283 102 Vimont, D. J., Battisti, D. S. & Hirst, A. C. Footprinting: A seasonal connection  
1284 between the tropics and mid-latitudes. *Geophysical Research Letters* **28**, 3923-3926  
1285 (2001). <https://doi.org/10.1029/2001GL013435>
- 1286 103 Capotondi, A. & Ricciardulli, L. The influence of pacific winds on ENSO diversity.  
1287 *Scientific Reports* **11**, 18672 (2021). <https://doi.org/10.1038/s41598-021-97963-4>
- 1288 104 XIE, S.-P. & PHILANDER, S. G. H. A coupled ocean-atmosphere model of relevance  
1289 to the ITCZ in the eastern Pacific. *Tellus A* **46**, 340-350 (1994).  
1290 <https://doi.org/10.1034/j.1600-0870.1994.t01-1-00001.x>
- 1291 105 Zhang, H., Clement, A. & Di Nezio, P. The South Pacific Meridional Mode: A  
1292 Mechanism for ENSO-like Variability. *Journal of Climate* **27**, 769-783 (2014).  
1293 <https://doi.org/10.1175/JCLI-D-13-00082.1>
- 1294 106 Chiang, J. C. H. & Vimont, D. J. Analogous Pacific and Atlantic meridional modes of  
1295 tropical atmosphere-ocean variability. *Journal of Climate* **17**, 4143-4158 (2004).  
1296 <https://doi.org/10.1175/Jcli4953.1>
- 1297 107 Amaya, D. J. *et al.* The North Pacific Pacemaker Effect on Historical ENSO and Its  
1298 Mechanisms. *Journal of Climate* **32**, 7643-7661 (2019). [https://doi.org/10.1175/Jcli-D-](https://doi.org/10.1175/Jcli-D-19-0040.1)  
1299 [19-0040.1](https://doi.org/10.1175/Jcli-D-19-0040.1)
- 1300 108 Anderson, B. T., Perez, R. C. & Karspeck, A. Triggering of El Niño onset through trade  
1301 wind-induced charging of the equatorial Pacific. *Geophysical Research Letters* **40**,  
1302 1212-1216 (2013). <https://doi.org/10.1002/grl.50200>
- 1303 109 Chakravorty, S. *et al.* Ocean Dynamics are Key to Extratropical Forcing of El Niño.  
1304 *Journal of Climate* **34**, 8739-8753 (2021). [https://doi.org/10.1175/JCLI-](https://doi.org/10.1175/JCLI-D-20-0933.1)  
1305 [D-20-0933.1](https://doi.org/10.1175/JCLI-D-20-0933.1)
- 1306 110 Hu, R., Lian, T., Feng, J. & Chen, D. Pacific Meridional Mode Does Not Induce Strong  
1307 Positive SST Anomalies in the Central Equatorial Pacific. *Journal of Climate* **36**, 4113-  
1308 4131 (2023). <https://doi.org/10.1175/JCLI-D-22-0503.1>



- 1309 111 Vimont, D. J., Alexander, M. A. & Newman, M. Optimal growth of Central and East  
1310 Pacific ENSO events. *Geophysical Research Letters* **41**, 4027-4034 (2014).  
1311 [https://doi.org:https://doi.org/10.1002/2014GL059997](https://doi.org/https://doi.org/10.1002/2014GL059997)
- 1312 112 Capotondi, A. & Sardeshmukh, P. D. Optimal precursors of different types of ENSO  
1313 events. *Geophysical Research Letters* **42** (2015).  
1314 [https://doi.org:https://doi.org/10.1002/2015GL066171](https://doi.org/https://doi.org/10.1002/2015GL066171)
- 1315 113 Di Lorenzo, E. *et al.* ENSO and meridional modes: A null hypothesis for Pacific climate  
1316 variability. *Geophysical Research Letters* **42**, 9440-9448 (2015).  
1317 <https://doi.org:10.1002/2015gl066281>
- 1318 114 Okumura, Y. M. Origins of Tropical Pacific Decadal Variability: Role of Stochastic  
1319 Atmospheric Forcing from the South Pacific. *Journal of Climate* **26**, 9791-9796 (2013).  
1320 [https://doi.org:https://doi.org/10.1175/JCLI-D-13-00448.1](https://doi.org/https://doi.org/10.1175/JCLI-D-13-00448.1)
- 1321 115 Zhao, Y. & Di Lorenzo, E. The impacts of Extra-tropical ENSO Precursors on Tropical  
1322 Pacific Decadal-scale Variability. *Scientific Reports* **10**, 3031 (2020).  
1323 <https://doi.org:10.1038/s41598-020-59253-3>
- 1324 116 Stuecker, M. F. Revisiting the Pacific Meridional Mode. *Scientific Reports* **8**, 3216  
1325 (2018). <https://doi.org:10.1038/s41598-018-21537-0>
- 1326 117 Sanchez, S. C., Amaya, D. J., Miller, A. J., Xie, S.-P. & Charles, C. D. The Pacific  
1327 Meridional Mode over the last millennium. *Climate Dynamics* **53**, 3547-3560 (2019).  
1328 <https://doi.org:10.1007/s00382-019-04740-1>
- 1329 118 McGregor, S., Holbrook, N. J. & Power, S. B. The Response of a Stochastically Forced  
1330 ENSO Model to Observed Off-Equatorial Wind Stress Forcing. *Journal of Climate* **22**,  
1331 2512-2525 (2009). [https://doi.org:https://doi.org/10.1175/2008JCLI2387.1](https://doi.org/https://doi.org/10.1175/2008JCLI2387.1)
- 1332 119 Liguori, G. & Di Lorenzo, E. Separating the North and South Pacific meridional modes  
1333 contributions to ENSO and tropical decadal variability. *Geophysical Research Letters*  
1334 **46**, 906-915 (2019).
- 1335 120 Chung, C. T. Y., Power, S. B., Sullivan, A. & Delage, F. The role of the South Pacific  
1336 in modulating Tropical Pacific variability. *Scientific Reports* **9**, 18311 (2019).  
1337 <https://doi.org:10.1038/s41598-019-52805-2>
- 1338 121 Sun, T. & Okumura, Y. M. Role of Stochastic Atmospheric Forcing from the South and  
1339 North Pacific in Tropical Pacific Decadal Variability. *Journal of Climate* **32**, 4013-  
1340 4038 (2019). [https://doi.org:https://doi.org/10.1175/JCLI-D-18-0536.1](https://doi.org/https://doi.org/10.1175/JCLI-D-18-0536.1)
- 1341 122 Lou, J., Holbrook, N. J. & O’Kane, T. J. South Pacific Decadal Climate Variability and  
1342 Potential Predictability. *Journal of Climate* **32**, 6051-6069 (2019).  
1343 [https://doi.org:https://doi.org/10.1175/JCLI-D-18-0249.1](https://doi.org/https://doi.org/10.1175/JCLI-D-18-0249.1)
- 1344 123 Capotondi, A., Newman, M., Xu, T. & Di Lorenzo, E. An Optimal Precursor of  
1345 Northeast Pacific Marine Heatwaves and Central Pacific El Niño Events. *Geophysical*  
1346 *Research Letters* **49**, e2021GL097350 (2022).  
1347 [https://doi.org:https://doi.org/10.1029/2021GL097350](https://doi.org/https://doi.org/10.1029/2021GL097350)

- 1348 124 Lorenzo, E. D. *et al.* Modes and Mechanisms of Pacific Decadal-Scale Variability.  
1349 *Annual Review of Marine Science* **15**, 249-275 (2023). [https://doi.org:10.1146/annurev-](https://doi.org:10.1146/annurev-marine-040422-084555)  
1350 [marine-040422-084555](https://doi.org:10.1146/annurev-marine-040422-084555)
- 1351 125 Zhao, Y., Newman, M., Capotondi, A., Di Lorenzo, E. & Sun, D. Removing the Effects  
1352 of Tropical Dynamics from North Pacific Climate Variability. *Journal of Climate* **34**,  
1353 9249-9265 (2021). <https://doi.org:https://doi.org/10.1175/JCLI-D-21-0344.1>
- 1354 126 Zhang, Y. *et al.* Atmospheric Forcing of the Pacific Meridional Mode: Tropical Pacific-  
1355 Driven Versus Internal Variability. *Geophysical Research Letters* **49**, e2022GL098148  
1356 (2022). <https://doi.org:https://doi.org/10.1029/2022GL098148>
- 1357 127 Stuecker, M. F. *et al.* Strong remote control of future equatorial warming by off-  
1358 equatorial forcing. *Nat Clim Change* **10**, 124-129 (2020).  
1359 <https://doi.org:10.1038/s41558-019-0667-6>
- 1360 128 Hazeleger, W., Severijns, C., Seager, R. & Molteni, F. Tropical Pacific–Driven Decadal  
1361 Energy Transport Variability. *Journal of Climate* **18**, 2037-2051 (2005).  
1362 <https://doi.org:https://doi.org/10.1175/JCLI3389.1>
- 1363 129 Farneti, R., Molteni, F. & Kucharski, F. Pacific interdecadal variability driven by  
1364 tropical–extratropical interactions. *Climate Dynamics* **42**, 3337-3355 (2014).  
1365 <https://doi.org:10.1007/s00382-013-1906-6>
- 1366 130 Cai, W. *et al.* Pantropical climate interactions. *Science* **363**, eaav4236 (2019).  
1367 <https://doi.org:doi:10.1126/science.aav4236>
- 1368 131 Johnson, H. L. & Marshall, D. P. Global Teleconnections of Meridional Overturning  
1369 Circulation Anomalies. *Journal of Physical Oceanography* **34**, 1702-1722 (2004).  
1370 [https://doi.org:https://doi.org/10.1175/1520-](https://doi.org:https://doi.org/10.1175/1520-0485(2004)034<1702:GTOMOC>2.0.CO;2)  
1371 [0485\(2004\)034<1702:GTOMOC>2.0.CO;2](https://doi.org:https://doi.org/10.1175/1520-0485(2004)034<1702:GTOMOC>2.0.CO;2)
- 1372 132 Gill, A. E. Some Simple Solutions for Heat-Induced Tropical Circulation. *Q J Roy*  
1373 *Meteor Soc* **106**, 447-462 (1980). <https://doi.org:DOI 10.1256/smsqj.44904>
- 1374 133 Polo, I., Martin-Rey, M., Rodriguez-Fonseca, B., Kucharski, F. & Mechoso, C. R.  
1375 Processes in the Pacific La Niña onset triggered by the Atlantic Niño. *Climate*  
1376 *Dynamics* **44**, 115-131 (2015). <https://doi.org:10.1007/s00382-014-2354-7>
- 1377 134 Li, X., Xie, S.-P., Gille, S. T. & Yoo, C. Atlantic-induced pan-tropical climate change  
1378 over the past three decades. *Nature Climate Change* **6**, 275-279 (2016).  
1379 <https://doi.org:10.1038/nclimate2840>
- 1380 135 Mochizuki, T., Kimoto, M., Watanabe, M., Chikamoto, Y. & Ishii, M. Interbasin effects  
1381 of the Indian Ocean on Pacific decadal climate change. *Geophysical Research Letters*  
1382 **43**, 7168-7175 (2016). <https://doi.org:https://doi.org/10.1002/2016GL069940>
- 1383 136 Kucharski, F. *et al.* Atlantic forcing of Pacific decadal variability. *Climate Dynamics*  
1384 **46**, 2337-2351 (2016). <https://doi.org:10.1007/s00382-015-2705-z>

- 1385 137 McGregor, S. *et al.* Recent Walker circulation strengthening and Pacific cooling  
1386 amplified by Atlantic warming. *Nature Climate Change* **4**, 888-892 (2014).  
1387 <https://doi.org:10.1038/nclimate2330>
- 1388 138 Chikamoto, Y., Mochizuki, T., Timmermann, A., Kimoto, M. & Watanabe, M.  
1389 Potential tropical Atlantic impacts on Pacific decadal climate trends. *Geophysical*  
1390 *Research Letters* **43**, 7143-7151 (2016).  
1391 <https://doi.org:https://doi.org/10.1002/2016GL069544>
- 1392 139 Chikamoto, Y. *et al.* Skilful multi-year predictions of tropical trans-basin climate  
1393 variability. *Nature Communications* **6**, 6869 (2015).  
1394 <https://doi.org:10.1038/ncomms7869>
- 1395 140 Luo, J.-J., Sasaki, W. & Masumoto, Y. Indian Ocean warming modulates Pacific  
1396 climate change. *Proceedings of the National Academy of Sciences* **109**, 18701-18706  
1397 (2012). <https://doi.org:doi:10.1073/pnas.1210239109>
- 1398 141 Sobel, A. H., Nilsson, J. & Polvani, L. M. The Weak Temperature Gradient  
1399 Approximation and Balanced Tropical Moisture Waves. *Journal of the Atmospheric*  
1400 *Sciences* **58**, 3650-3665 (2001). [https://doi.org:https://doi.org/10.1175/1520-0469\(2001\)058<3650:TWTGAA>2.0.CO;2](https://doi.org:https://doi.org/10.1175/1520-0469(2001)058<3650:TWTGAA>2.0.CO;2)
- 1402 142 Bretherton, C. S. & Sobel, A. H. The Gill Model and the Weak Temperature Gradient  
1403 Approximation. *Journal of the Atmospheric Sciences* **60**, 451-460 (2003).  
1404 [https://doi.org:https://doi.org/10.1175/1520-0469\(2003\)060<0451:TGMATW>2.0.CO;2](https://doi.org:https://doi.org/10.1175/1520-0469(2003)060<0451:TGMATW>2.0.CO;2)
- 1406 143 Chiang, J. C. H. & Sobel, A. H. Tropical Tropospheric Temperature Variations Caused  
1407 by ENSO and Their Influence on the Remote Tropical Climate. *Journal of Climate* **15**,  
1408 2616-2631 (2002). [https://doi.org:https://doi.org/10.1175/1520-0442\(2002\)015<2616:TTVCB>2.0.CO;2](https://doi.org:https://doi.org/10.1175/1520-0442(2002)015<2616:TTVCB>2.0.CO;2)
- 1410 144 Sun, C. *et al.* Western tropical Pacific multidecadal variability forced by the Atlantic  
1411 multidecadal oscillation. *Nature Communications* **8**, 15998 (2017).  
1412 <https://doi.org:10.1038/ncomms15998>
- 1413 145 Johnson, Z. F., Chikamoto, Y., Wang, S. Y. S., McPhaden, M. J. & Mochizuki, T.  
1414 Pacific decadal oscillation remotely forced by the equatorial Pacific and the Atlantic  
1415 Oceans. *Climate Dynamics* **55**, 789-811 (2020). <https://doi.org:10.1007/s00382-020-05295-2>
- 1417 146 Xie, S.-P., Okumura, Y., Miyama, T. & Timmermann, A. Influences of Atlantic  
1418 Climate Change on the Tropical Pacific via the Central American Isthmus. *Journal of*  
1419 *Climate* **21**, 3914-3928 (2008). <https://doi.org:https://doi.org/10.1175/2008JCLI2231.1>
- 1420 147 Orihuela-Pinto, B., England, M. H. & Taschetto, A. S. Interbasin and interhemispheric  
1421 impacts of a collapsed Atlantic Overturning Circulation. *Nature Climate Change* **12**,  
1422 558-565 (2022). <https://doi.org:10.1038/s41558-022-01380-y>
- 1423 148 Ham, Y.-G., Kug, J.-S., Park, J.-Y. & Jin, F.-F. Sea surface temperature in the north  
1424 tropical Atlantic as a trigger for El Niño/Southern Oscillation events. *Nature*  
1425 *Geoscience* **6**, 112-116 (2013). <https://doi.org:10.1038/ngeo1686>

- 1426 149 Dhame, S., Taschetto, A. S., Santoso, A. & Meissner, K. J. Indian Ocean warming  
1427 modulates global atmospheric circulation trends. *Climate Dynamics* **55**, 2053-2073  
1428 (2020). <https://doi.org:10.1007/s00382-020-05369-1>
- 1429 150 Kucharski, F. *et al.* The Teleconnection of the Tropical Atlantic to Indo-Pacific Sea  
1430 Surface Temperatures on Inter-Annual to Centennial Time Scales: A Review of Recent  
1431 Findings. *Atmosphere* **7**, 29 (2016).
- 1432 151 Ruprich-Robert, Y. *et al.* Assessing the Climate Impacts of the Observed Atlantic  
1433 Multidecadal Variability Using the GFDL CM2.1 and NCAR CESM1 Global Coupled  
1434 Models. *Journal of Climate* **30**, 2785-2810 (2017).  
1435 <https://doi.org:https://doi.org/10.1175/JCLI-D-16-0127.1>
- 1436 152 Ruprich-Robert, Y. *et al.* Impacts of Atlantic multidecadal variability on the tropical  
1437 Pacific: a multi-model study. *npj Climate and Atmospheric Science* **4**, 33 (2021).  
1438 <https://doi.org:10.1038/s41612-021-00188-5>
- 1439 153 Hu, S. & Fedorov, A. V. Cross-equatorial winds control El Niño diversity and change.  
1440 *Nature Climate Change* **8**, 798-802 (2018). [https://doi.org:10.1038/s41558-018-0248-](https://doi.org:10.1038/s41558-018-0248-0)  
1441 [0](https://doi.org:10.1038/s41558-018-0248-0)
- 1442 154 Dong, L. & McPhaden, M. J. The Effects of External Forcing and Internal Variability  
1443 on the Formation of Interhemispheric Sea Surface Temperature Gradient Trends in the  
1444 Indian Ocean. *Journal of Climate* **30**, 9077-9095 (2017).  
1445 <https://doi.org:https://doi.org/10.1175/JCLI-D-17-0138.1>
- 1446 155 Kajtar, J. B., Santoso, A., England, M. H. & Cai, W. Tropical climate variability:  
1447 interactions across the Pacific, Indian, and Atlantic Oceans. *Climate Dynamics* **48**,  
1448 2173-2190 (2017). <https://doi.org:10.1007/s00382-016-3199-z>
- 1449 156 Terray, P., Masson, S., Prodhomme, C., Roxy, M. K. & Sooraj, K. P. Impacts of Indian  
1450 and Atlantic oceans on ENSO in a comprehensive modeling framework. *Climate*  
1451 *Dynamics* **46**, 2507-2533 (2016). <https://doi.org:10.1007/s00382-015-2715-x>
- 1452 157 Meehl, G. A. *et al.* Atlantic and Pacific tropics connected by mutually interactive  
1453 decadal-timescale processes. *Nature Geoscience* **14**, 36-42 (2021).  
1454 <https://doi.org:10.1038/s41561-020-00669-x>
- 1455 158 O'Reilly, C. H. *et al.* Challenges with interpreting the impact of Atlantic Multidecadal  
1456 Variability using SST-restoring experiments. *npj Climate and Atmospheric Science* **6**,  
1457 14 (2023). <https://doi.org:10.1038/s41612-023-00335-0>
- 1458 159 Penland, C. & Sardeshmukh, P. D. The Optimal-Growth of Tropical Sea-Surface  
1459 Temperature Anomalies. *Journal of Climate* **8**, 1999-2024 (1995). <https://doi.org:Doi>  
1460 [10.1175/1520-0442\(1995\)008<1999:Togots>2.0.Co;2](https://doi.org:10.1175/1520-0442(1995)008<1999:Togots>2.0.Co;2)
- 1461 160 Zhao, Y., Newman, M., Capotondi, A., Di Lorenzo, E. & Sun, D. Removing the Effects  
1462 of Tropical Dynamics from North Pacific Climate Variability. *Journal of Climate*, 1-  
1463 49 (2021). <https://doi.org:10.1175/JCLI-D-21-0344.1>

- 1464 161 Zhao, Y., Jin, Y., Li, J. & Capotondi, A. The Role of Extratropical Pacific in Crossing  
1465 ENSO Spring Predictability Barrier. *Geophysical Research Letters* **49**,  
1466 e2022GL099488 (2022). <https://doi.org/10.1029/2022GL099488>
- 1467 162 Zhao, Y., Jin, Y., Capotondi, A., Li, J. & Sun, D. The Role of Tropical Atlantic in  
1468 ENSO Predictability Barrier. *Geophysical Research Letters* **50**, e2022GL101853  
1469 (2023). <https://doi.org/10.1029/2022GL101853>
- 1470 163 Qiu, B. & Chen, S. Interannual-to-Decadal Variability in the Bifurcation of the North  
1471 Equatorial Current off the Philippines. *Journal of Physical Oceanography* **40**, 2525-  
1472 2538 (2010). <https://doi.org/10.1175/2010JPO4462.1>
- 1473 164 Capotondi, A., Alexander, M. A., Bond, N. A., Curchitser, E. N. & Scott, J. D.  
1474 Enhanced upper ocean stratification with climate change in the CMIP3 models. *Journal*  
1475 *of Geophysical Research: Oceans* **117** (2012).  
1476 <https://doi.org/10.1029/2011JC007409>
- 1477 165 Geng, T., Yang, Y. & Wu, L. On the Mechanisms of Pacific Decadal Oscillation  
1478 Modulation in a Warming Climate. *Journal of Climate* **32**, 1443-1459 (2019).  
1479 <https://doi.org/10.1175/JCLI-D-18-0337.1>
- 1480 166 Xu, Y. & Hu, A. How Would the Twenty-First-Century Warming Influence Pacific  
1481 Decadal Variability and Its Connection to North American Rainfall: Assessment Based  
1482 on a Revised Procedure for the IPO/PDO. *Journal of Climate* **31**, 1547-1563 (2018).  
1483 <https://doi.org/10.1175/JCLI-D-17-0319.1>
- 1484 167 Jia, F. *et al.* Weakening Atlantic Niño-Pacific connection under  
1485 greenhouse warming. *Science Advances* **5**, eaax4111 (2019).  
1486 <https://doi.org/10.1126/sciadv.aax4111>
- 1487 168 Jia, F., Cai, W., Gan, B., Wu, L. & Di Lorenzo, E. Enhanced North Pacific impact on  
1488 El Niño/Southern Oscillation under greenhouse warming. *Nature Climate Change* **11**,  
1489 840-847 (2021). <https://doi.org/10.1038/s41558-021-01139-x>
- 1490 169 Liguori, G. & Di Lorenzo, E. Meridional Modes and Increasing Pacific Decadal  
1491 Variability Under Anthropogenic Forcing. *Geophysical Research Letters* **45**, 983-991  
1492 (2018). <https://doi.org/10.1002/2017GL076548>
- 1493 170 Hu, D. *et al.* Pacific western boundary currents and their roles in climate. *Nature* **522**,  
1494 299-308 (2015). <https://doi.org/10.1038/nature14504>
- 1495 171 Cobb, K. M., Charles, C. D., Cheng, H. & Edwards, R. L. El Niño/Southern Oscillation  
1496 and tropical Pacific climate during the last millennium. *Nature* **424**, 271-276 (2003).  
1497 <https://doi.org/10.1038/nature01779>
- 1498 172 Ramos, R. D., Goodkin, N. F., Siringan, F. P. & Hughen, K. A. Coral Records of  
1499 Temperature and Salinity in the Tropical Western Pacific Reveal Influence of the  
1500 Pacific Decadal Oscillation Since the Late Nineteenth Century. *Paleoceanography and*  
1501 *Paleoclimatology* **34**, 1344-1358 (2019).  
1502 <https://doi.org/10.1029/2019PA003684>

- 1503 173 Nurhati, I. S., Cobb, K. M. & Di Lorenzo, E. Decadal-Scale SST and Salinity Variations  
1504 in the Central Tropical Pacific: Signatures of Natural and Anthropogenic Climate  
1505 Change. *Journal of Climate* **24**, 3294-3308 (2011).  
1506 [https://doi.org:https://doi.org/10.1175/2011JCLI3852.1](https://doi.org/https://doi.org/10.1175/2011JCLI3852.1)
- 1507 174 Sanchez, S. C., Charles, C. D., Carriquiry, J. D. & Villaescusa, J. A. Two centuries of  
1508 coherent decadal climate variability across the Pacific North American region.  
1509 *Geophysical Research Letters* **43**, 9208-9216 (2016).  
1510 <https://doi.org:https://doi.org/10.1002/2016GL069037>
- 1511 175 Dassié, E. P., Hasson, A., Khodri, M., Lebas, N. & Linsley, B. K. Spatiotemporal  
1512 Variability of the South Pacific Convergence Zone Fresh Pool Eastern Front from  
1513 Coral-Derived Surface Salinity Data. *Journal of Climate* **31**, 3265-3288 (2018).  
1514 <https://doi.org:https://doi.org/10.1175/JCLI-D-17-0071.1>
- 1515 176 Thompson, D. M., Cole, J. E., Shen, G. T., Tudhope, A. W. & Meehl, G. A. Early  
1516 twentieth-century warming linked to tropical Pacific wind strength. *Nature Geoscience*  
1517 **8**, 117-121 (2015). <https://doi.org:10.1038/ngeo2321>
- 1518 177 Guilderson, T. P. & Schrag, D. P. Abrupt Shift in Subsurface Temperatures in the  
1519 Tropical Pacific Associated with Changes in El Niño. *Science* **281**, 240-243  
1520 (1998). <https://doi.org:doi:10.1126/science.281.5374.240>
- 1521 178 Druffel, E. R. M. *et al.* Seasonal radiocarbon and oxygen isotopes in a Galapagos coral:  
1522 Calibration with climate indices. *Geophysical Research Letters* **41**, 5099-5105 (2014).  
1523 <https://doi.org:https://doi.org/10.1002/2014GL060504>
- 1524 179 Abram, N. J. *et al.* Coupling of Indo-Pacific climate variability over the last  
1525 millennium. *Nature* **579**, 385-392 (2020). <https://doi.org:10.1038/s41586-020-2084-4>
- 1526 180 Cobb, K. M., Charles, C. D. & Hunter, D. E. A central tropical Pacific coral  
1527 demonstrates Pacific, Indian, and Atlantic decadal climate connections. *Geophysical*  
1528 *Research Letters* **28**, 2209-2212 (2001).  
1529 <https://doi.org:https://doi.org/10.1029/2001GL012919>
- 1530 181 Bechtold, B. Violin Plots for Matlab, Github Project. (2016).  
1531 <https://doi.org:10.5281/zenodo.4559847>
- 1532 182 Huang, B. Y. *et al.* Extended Reconstructed Sea Surface Temperature, Version 5  
1533 (ERSSTv5): Upgrades, Validations, and Intercomparisons. *Journal of Climate* **30**,  
1534 8179-8205 (2017). <https://doi.org:10.1175/Jcli-D-16-0836.1>
- 1535 183 Kalnay, E. *et al.* The NCEP/NCAR 40-Year Reanalysis Project. *Bulletin of the*  
1536 *American Meteorological Society* **77**, 437-472 (1996).  
1537 [https://doi.org:https://doi.org/10.1175/1520-0477\(1996\)077<0437:TNYRP>2.0.CO;2](https://doi.org:https://doi.org/10.1175/1520-0477(1996)077<0437:TNYRP>2.0.CO;2)
- 1538 184 Zuo, H., Balmaseda, M. A., Tietsche, S., Mogensen, K. & Mayer, M. The ECMWF  
1539 operational ensemble reanalysis–analysis system for ocean and sea ice: a description of  
1540 the system and assessment. *Ocean Sci.* **15**, 779-808 (2019). [https://doi.org:10.5194/os-](https://doi.org:10.5194/os-15-779-2019)  
1541 [15-779-2019](https://doi.org:10.5194/os-15-779-2019)

- 1542 185 Balmaseda, M. A., Mogensen, K. & Weaver, A. T. Evaluation of the ECMWF ocean  
1543 reanalysis system ORAS4. *Q J Roy Meteor Soc* **139**, 1132-1161 (2013).  
1544 [https://doi.org:https://doi.org/10.1002/qj.2063](https://doi.org/https://doi.org/10.1002/qj.2063)
- 1545 186 Behringer, D. & Xue, Y. Evaluation of the global ocean data assimilation system at  
1546 NCEP: The Pacific Ocean. 11-15 (2004).
- 1547 187 Carton, J. A. & Giese, B. S. A Reanalysis of Ocean Climate Using Simple Ocean Data  
1548 Assimilation (SODA). *Mon Weather Rev* **136**, 2999-3017 (2008).  
1549 <https://doi.org:https://doi.org/10.1175/2007MWR1978.1>
- 1550 188 Zuo, H., Balmaseda, M. A. & Mogensen, K. The new eddy-permitting ORAP5 ocean  
1551 reanalysis: description, evaluation and uncertainties in climate signals. *Climate*  
1552 *Dynamics* **49**, 791-811 (2017). <https://doi.org:10.1007/s00382-015-2675-1>
- 1553 189 You, Y. & Furtado, J. C. The South Pacific Meridional Mode and Its Role in Tropical  
1554 Pacific Climate Variability. *Journal of Climate* **31**, 10141-10163 (2018).  
1555 <https://doi.org:https://doi.org/10.1175/JCLI-D-17-0860.1>
- 1556 190 Naha, R., McGregor, S. & Singh, M. Exploring the symmetries of pan-tropical  
1557 connections between the tropical Atlantic and Pacific basins. *Journal of Climate*, 1-34  
1558 (2023). <https://doi.org:https://doi.org/10.1175/JCLI-D-22-0355.1>  
1559